1   **Spatio-temporal diversity of dietary preferences and stress sensibilities of early and middle**

2   **Miocene Rhinocerotidae from Eurasia: impact of climate changes**

3

4

5   Authors: M. Hullot[1], G. Merceron[2], P.-O. Antoine[3]

6

7   1- Bayerische Staatssammlung für Paläontologie und Geologie, Richard-Wagner Straße 10,

8   80333 Munich, Germany

9   2- PALEVOPRIM UMR 7262, CNRS, Université de Poitiers, 86073 Poitiers, France

10   3- Institut des Sciences de l'Évolution, UMR5554, Univ Montpellier, CNRS, IRD, Place Eugène

11   Bataillon, CC064, 34095 Montpellier, France

12

13   **Abstract**

14

15   Major climatic and ecological changes are documented in terrestrial ecosystems during the Miocene

16   epoch. The Rhinocerotidae are a very interesting clade to investigate the impact of these changes on

17   ecology, as they are abundant and diverse in the fossil record throughout the Miocene. Here, we

18   explored the spatio-temporal evolution of rhinocerotids' paleoecology during the early and middle

19   Miocene in Europe and Pakistan. We studied the dental texture microwear (proxy for diet) and enamel

20   hypoplasia (stress indicator) of 19 species belonging to four sub-tribes and an unnamed clade of

21   Rhinocerotidae, and coming from nine Eurasian localities ranging from MN2 to MN7/8. Our results

22   suggest a clear niche partitioning based on diet at Kumbi 4 (MN2, Pakistan), Sansan (MN6, France),

23   and Villefranche d'Astarac (MN7/8, France), while dietary overlap and subtle variations are discussed

24   for Béon 1 (MN4, France) and Gračanica (MN5/6, Bosnia-Herzegovina). All rhinocerotids studied were

25   browsers or mixed-feeders, and none had a grazing nor frugivore diet. Regarding hypoplasia, the

26   prevalence was moderate (~ 10%) to high (> 20 %) at all localities but Kumbi 4 (~ 6 %), and

27   documented quite well the local conditions. Sansan and Devínska Nová Ves (MN6, Slovakia), both

28   dated to the MN6 (i.e., by the middle Miocene Climatic Transition, ca. 13.9 Mya), had moderate

29   hypoplasia prevalence. Besides locality, species and tooth locus were also important factors of

30   variation for the prevalence of hypoplasia. The very large hippo-like *Brachypotherium brachypus* was

31   one of the most affected species at all concerned localities (but Sansan), while early-diverging

32   elasmotheriines were very little affected.

33

34   **Keywords**: paleoecology, Miocene Climatic Optimum (MCO), microwear (DMTA), enamel hypoplasia

35

36   **Introduction**

37

38   The Miocene is a key period in Earth and rhinocerotid evolutionary histories. Climatic conditions in

39   Eurasia during the Miocene epoch are globally tropical and the typical habitat is forested (Cerling et

40   al., 1997; Zachos et al., 2001; Bruch et al., 2007; Westerhold et al., 2020). It is the last warm episode

41   of the Cenozoic era, although marked by great climatic changes prefiguring the setup of modern cold

42   conditions (Westerhold et al., 2020). During early Miocene times, temperatures increased until

43   reaching the Miocene Climatic Optimum (MCO) between ~17 to 14 Mya (corresponding to the late

44   Burdigalian + Langhian standard ages; Westerhold et al., 2020). This optimum is followed by an

45   abrupt cooling (the middle Miocene climatic transition [mMCT]; Westerhold et al., 2020) associated

46   with faunal turnovers in Eurasia (Böhme, 2003; Maridet et al., 2007). The middle Miocene is marked

47   by a relative aridity, associated with a global cooling (Bruch et al., 2007; Böhme et al., 2008).

48

49   Concerning rhinocerotids, Miocene times witness peaks in their alpha diversity about 22–18 Mya and

50   11–10 Mya (Antoine et al., 2010; Antoine and Becker, 2013; Antoine, in press). During the early and

51   middle Miocene in Eurasia, four sub-tribes of Rhinocerotidae are encountered – Rhinocerotina,

52   Teleoceratina and Aceratheriina (Rhinocerotinae), and Elasmotheriina (Elasmotheriinae) – and

53   species of which are often found associated in fossil-yielding localities (Antoine et al., 1997, 2010;

54   Heissig, 2012; Becker and Tissier, 2020; Antoine, 2002, in press). This abundance and the potential

55   cohabitation of such large herbivores question habitat capacity and competition for food resources.

56   However, the ecology of the rhinocerotids has rarely been explored or only been assumed based on

57   morphological adaptations (Prothero et al., 1989; Prothero, 2005; Giaourtsakis et al., 2006). If the

58   Rhinocerotina appear to be ecologically varied, the literature suggests a similar ecology for most

59   elasmotheriines on one hand, as open environment dwellers adapted to though vegetation (Iñigo and

60   Cerdeño, 1997; Antoine and Welcomme, 2000), and for the teleoceratines on another hand, as hippo-

61   like rhinoceroses inhabiting lake side or swamps and probably browsing on low vegetation or even

62   grazing (Prothero et al., 1989; Cerdeño, 1998).

63

64   In this article, we focused on the rhinocerotids from nine localities, covering wide temporal and

65   geographical ranges (from MN2 to MN7/8 and from southwestern France to Pakistan). We assessed

66   dietary preferences using dental microwear texture analysis, and stress sensibility via the study of

67   enamel hypoplasia.

68

69   **Material and methods**

70

71   We studied the rhinocerotid dental remains from nine early and middle Miocene localities from France

72   (Béon 1, Béon 2, Sansan, Simorre, and Villefranche d'Astarac), Germany (Steinheim am Albuch),

73   Bosnia-Herzegovina (Gračanica), Slovakia (Devínska Nová Ves Spalte), and Pakistan (Kumbi 4,

74   Balochistan), ranging from MN2 to MN7/8. The rhinocerotid assemblages are detailed in Table 1. The

75   specimens are curated at the Naturhistorisches Museum Wien (NHMW), the Muséum de Toulouse

76   (MHNT), and the Naturhistorisches Museum Basel (NHMB). For all details on the specimens included

77   in this study see Supplementary S1. The localization of the studied localities is given in Figure 1.

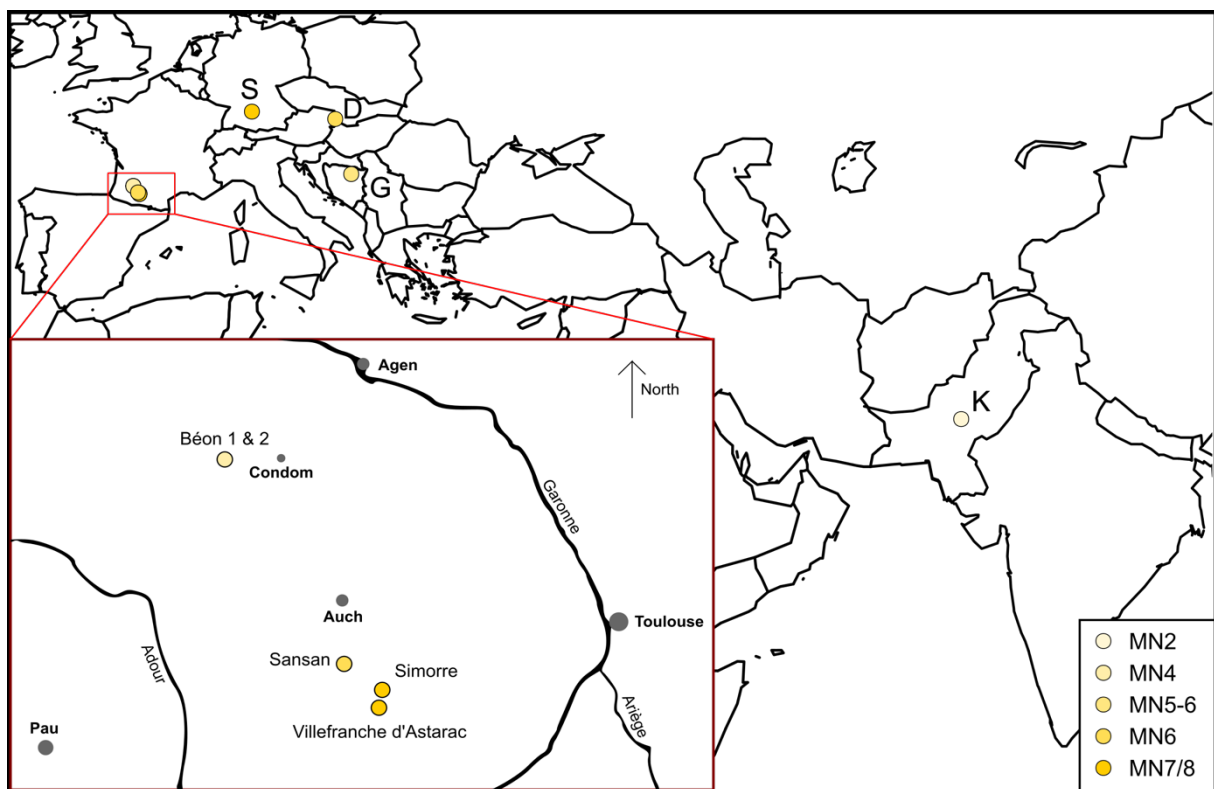78   Further details on the localities are given in Supplementary S2.

79

80   Dental Microwear Texture Analyses (DMTA)

81   Dental Microwear Texture Analysis (DMTA) is a powerful approach to characterize dietary preferences

82   at a short time scale (days to weeks prior the death of the individual; Hoffman et al., 2015; Winkler et

83   al., 2020), widely used in paleontological and archeological studies (Grine, 1986; Rivals et al., 2012;

84   Jones and DeSantis, 2017; Berlioz et al., 2018). We studied dental microwear texture on one well-

85   preserved molar (germs and over-worn teeth excluded) per individual, preferentially the second molar

86   (first or third otherwise), either upper or lower, left or right.

87

88   After cleaning the tooth with acetone or ethanol, two silicone (Regular Body President, ref. 6015 - ISO

89   4823, medium consistency, polyvinylsiloxane addition type; Coltene Whaledent) molds were made on

90   a single enamel band, which shows two different facets acting as grinding and shearing (if present).

91   This shearing facet has a steep slope while the former is more horizontal and show several HSB band

92   on the very enamel surface. To combine both type of facets with different functions indeed improves

93   dietary reconstruction (Louail et al., 2021; Merceron et al., 2021). The enamel band on which we

94   identified those two facets is localized labially near the protocone on upper molars and distally to the

95   protoconid or hypoconid (if the protoconid is unavailable) on lower teeth (see supplementary S2).

96

97

99   **Figure 1: Geographical position of the studied Eurasian Miocene localities.**

100   Localization of all localities in Eurasia. Red square is a zoom on the southwestern French localities,

101   modified from Antoine and Duranthon (1997).

102   Color code by MN zones as detailed in A. Abbreviations from West to East: S- Steinheim am Albuch

103   (MN7/8; Germany), D- Devínska Nová Ves Spalte (MN6; Slovakia), G- Gračanica (MN5-6; Bosnia-

104   Herzegovina), K- Kumbi 4 (MN2; Pakistan).

4

Table 1: List of rhinocerotid species found at each locality studied

	Kumbi 4	Béon 2	Béon 1	Gračanica	Sansan	Devínska Nová Ves Spalte	Steinheim am Albuch	Simorre	Villefranche d'Astarac
Rhinocerotinae									
Mesaceratherium welcommi	x								
Pleuroceros blanfordi	x								
Protaceratherium sp.	x								
Protaceratherium minutum		x							
Plesiaceratherium naricum	x								
Plesiaceratherium mirallesi		x	x						
Plesiaceratherium balkanicum					x		x		
Plesiaceratherium sp.				x					
Aceratheriina									
Hoploaceratherium tetradactylum					x				
Alicornops simorrense					x			x	x	x
Rhinocerotina									
Gaindatherium cf. *browni*	x								
Lartetotherium sansaniense				x	x		x		
Dicerorhinus steinheimensis						x	x		
Teleoceratina									
Brachypotherium brachypus			x	x	x		x	x	x
Brachypotherium gajense	x								
Diaceratherium fatehjangense	x								
Prosantorhinus douvillei		aff.	x						
Prosantorhinus shahbazi	x								
Elasmotheriinae									
Elasmotheriina									
Bugtirhinus praecursor	x								
Hispanotherium beonense			x						
Hispanotherium cf. *matritense*					x				
Total	9	3	5	4	4	2	4	2	2

In this article we followed a protocol adapted from Scott et al. (2005, 2006) with sensitive-scale fractal

analyses. Molds were scanned with a Leica DCM8 confocal profilometer ("TRIDENT" profilometer

housed at the PALEVOPRIM, CNRS, University of Poitiers) using white light confocal technology with

a 100× objective (Leica Microsystems; Numerical aperture: 0.90; working distance: 0.9 mm). The

112 obtained scans (.plu files) were pre-treated with LeicaMap v.8.2. (Leica Microsystems) as follows: the

113 surface was inverted (as scans were made on negative replicas), missing points (i.e., non-measured,

114 less than 1%) were replaced by the mean of the neighboring points and aberrant peaks were removed

115 (see details in the supplementary Information in Merceron et al., 2016b). The surface was then

116 levelled, and we applied a polynomial of degree 8 removal of form to temper for Hunter-Schreger

117 bands reliefs in the DMTA parameters. Eventually, we selected a 200×200-µm area (1551 × 1551

118 pixels) within the surface, which we saved as a digital elevation model (.sur) and used to extract

119 DMTA parameters through Scale-Sensitive Fractal Analysis with SFrax (Surfract, www.surfract.com)

120 and LeicaMap.

121

122 Here we focused on five classical DMTA parameters: anisotropy (exact proportion of length-scale

123 anisotropy of relief; epLsar), complexity (area-scale fractal complexity; Asfc), heterogeneity of

124 complexity (heterogeneity of area-scale fractal complexity here at 3×3 and 9×9; HAsfc9 and HAsfc81),

125 and fine textural fill volume (here at 0.2 µm; FTfv). The description of theses parameters is available in

126 Scott et al. (2006).

127

128 To facilitate DMTA interpretation for fossil specimen, we used specimens of the five extant rhinocerotid

129 species. This extant dataset was modified from that of Hullot et al. (2019), as precised below, and

130 consists of 17 specimens of *Ceratotherium simum* (white rhinoceros), four of *Dicerorhinus sumatrensis*

131 (Sumatran rhinoceros), 21 of Diceros bicornis (black rhinoceros), 15 of *Rhinoceros sondaicus* (Javan

132 rhinoceros; one new specimen), and five of *Rhinoceros unicornis* (Indian rhinoceros; one new
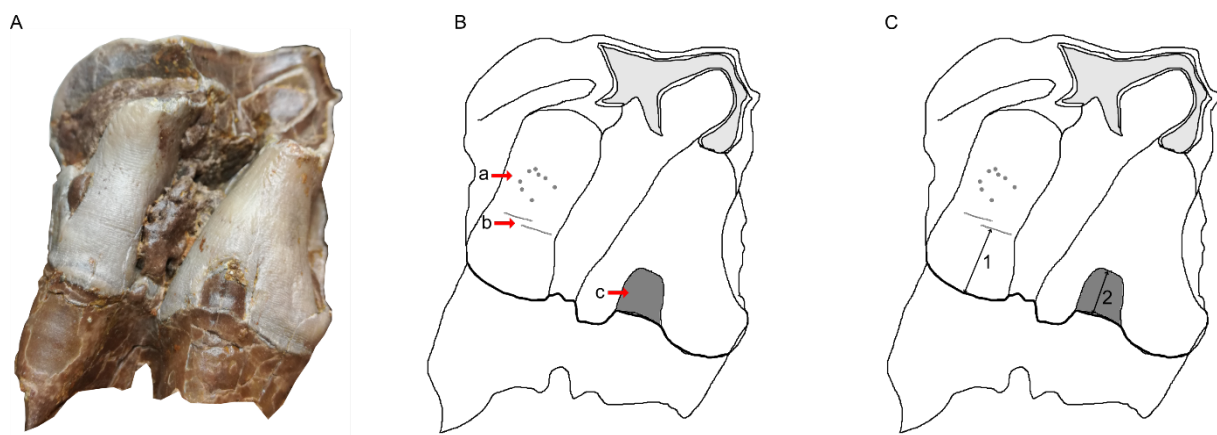
133 specimen).

134

135 <u>Enamel hypoplasia</u>

136 Hypoplasia is a common defect of the enamel resulting from a stress or a combination of stresses

137 occurring during tooth development (Goodman and Rose, 1990). It is a permanent, sensitive, but non-

138 specific indicator of stresses either environmental (e.g., drought or nutritional stress; Skinner and

139 Pruetz, 2012; Upex and Dobney, 2012), physiological (e.g., disease or parasitism; Suckling et al.,

140 1986; Rothschild et al., 2001; Niven et al., 2004), and/or psychological (e.g., depression in primates;

141 Guatelli-Steinberg, 2001).

142 Enamel hypoplasia was studied with the naked eye and categorization of the defects followed the

143 *Fédération Dentaire Internationale* (1982) as linear enamel hypoplasia (LEH), pitted hypoplasia, or

144 aplasia. We studied all cheek teeth, both deciduous and permanent, but excluded 62 teeth to avoid

145 false negative and uncalibrated defects, as enamel was obscured (e.g., tooth unerupted in bone,

146 sediment occluding), broken or worn out, or as identification was impossible. This left 1401 teeth

147 studied for the hypoplasia analysis – 294 milk molars and 1107 permanent premolars and molars –

148 from the nine localities. In parallel, qualitative data (tooth locus affected, position of the defect on the

149 crown, and severity) and caliper measurements (distance of the defect from enamel-dentine junction,

150 width if applicable) were taken (details in Supplementary S3). Type of defects recorded, and caliper

151 measurements are illustrated in Figure 2.

152

153

154

155

156 **Figure 2: The three different types of hypoplasia considered in this study and the associated**

157 **measurements**

158 A- Lingual view of right M2 of the specimen MHNT.PAL.2004.0.58 (*Hispanotherium beonense*)

159 displaying three types of hypoplasia

160 B- Interpretative drawing of the photo in A illustrating the hypoplastic defects: a- pitted hypoplasia, b-

161 linear enamel hypoplasia, and c- aplasia

162 C- Interpretative drawing of the photo in A illustrating the measurements: 1- distance between the

163 base of the defect and the enamel-dentin junction, 2- width of the defect (when applicable).

164 Figure from Hullot et al. (2021).

165

166 <u>Statistics and GLMMs</u>

167 Statistics were conducted in R (R Core Team, 2018: https://www.R-project.org/), equipped with the

168 following packages: reshape2 (Wickham, 2007), dplyr (Wickham et al., 2019), lme4 (Bates et al.,

169 2015), car (Fox et al., 2012), MASS (Venables and Ripley, 2002). According to the recent statement of

170 the American Statistical Association (ASA) on p-values (Wasserstein and Lazar, 2016; Wasserstein et

171 al., 2019), we avoided the use of the term "statistically significant" in this manuscript and the classical

172 thresholds as much as possible. Figures were done using R package ggplot2 (Wickham, 2011) as well

173 as Inkscape v.0.91.

174

175 General Linear Mixed Models (GLMM) on our data were constructed based on a R code modified from

176 Arman et al. (2019) and adapted to each tested response variable. An example of this code applied to

177 hypoplasia variable Hypo is given in Supplementary 4. DMTA response variables were the five DMTA

178 parameters (epLsar, Asfc, FTfv, HAsfc9, and HAsfc81) and we selected Gaussian family for the

179 GLMMs. Factors in the models were: specimen (number of the specimen; random factor), locality,

180 province, age (MN zones), genus, tooth (e.g., second molar, fourth milk molar), position (upper or

181 lower), side (left or right), cusp (protocone, protoconid, hypoconid), and facet (grinding or shearing).

182 For hypoplasia, response variables were Hypo (1 or 0 for presence or absence of hypoplasia,

183 respectively) for which we used Binomial family, Defect (e.g., LEH, Pits, Aplasia; converted to

184 numbers), Localization (position of the defect on the crown; mostly labial or lingual), Multiple (number

185 of defects), and Severity (0 to 4), modeled using Poisson family. The factors were: specimen (number

186 of the specimen; random factor), locality, province, age (MN zones), genus, tooth (e.g., first molar,

187 fourth premolar), position (upper or lower), side (left or right), and wear (low, average, high).

188 Additionally, for response variables Severity, Multiple, and Localization, defect was converted and

189 used as a factor.

190

191 The models were built with a bottom-up approach, starting with the only random factor of our dataset

192 alone (specimen) and adding factors incrementally for every set (e.g., 1|Specimen + Genus,

193 1|Specimen + Locality). New set was built has long as Akaike's Information Criterion score (AIC) kept

194 decreasing. Few interactions (e.g., Genus x Facet for microwear, Genus x Tooth for hypoplasia) were

195 considered in the models, as most factors were considered independent and to avoid unnecessarily

8

196   complex and rarely selected models (Arman et al., 2019). We selected the best candidate model as

197   the one with the lowest AIC and checked for over-dispersion (estimated through the ratio of deviance

198   and degrees of freedom). If needed, we corrected it through quasi-Poisson or quasi-Binomial laws

199   from the MASS package (Venables and Ripley, 2002) or by adjusting the coefficients table (multiply

200   type error by square root of the dispersion factor and recalculate Z and p values accordingly). In total,

201   340 models were compared across the 10 response variables (see electronic supplementary material,

202   S5, S6, and S7).

203

204   **Results**

205

206   <u>Microwear</u>

207   MANOVA (Species x Facet x Age x Locality) on all five main DMTA parameters (epLsar, Asfc, FTfv,

208   HAsfc9, HAsfc81) revealed low p-values for Species (df = 14; p-value = 8.6×10^{-4}), Facet (df = 1; p-

209   value = 6.5×10^{-4}), and Locality (df = 4; p-value = 0.014). The ANOVAs for each parameter,

210   highlighted at least a marked influence of Species (all parameters; p-values between 7.3×10^{-4} and

211   0.027), Facet (Asfc, p-value = 0.028; FTfv, p-value = 6.22×10^{-6}), Age (Asfc, p-value = 7.57×10^{-3}), or

212   Locality (epLsar, p-value = 0.01; Asfc, p-value = 1.7×10^{-4}). To precise the differences for Species and

213   Locality (factors with more than two states) we ran post hocs, results of which are detailed in Table 2

214   and Table 3. The more conservative post hoc (Tukey's honestly significant difference; HSD) revealed

215   very few noticeable differences in the microwear textures of the studied rhinocerotid specimens by

216   Species or Locality (low p-values relatively to other pairs; Table 2). The DMT of *Hoploaceratherium*

217   *tetradactylum* appears quite distinct from that of *Plesiaceratherium* spp. (epLsar, Asfc, HAsfc9 and

218   HAfsc81). Concerning Locality, Gračanica specimens stood out with very low values of complexity

219   compared to Sansan (p-value = 0.047), Simorre (p-value = 0.028), and Villefranche d'Astarac (p-value

220   = 0.032).

221

222   The least conservative post hoc (Fischer's least significant difference; LSD) highlighted more

223   differences in the DMTA patterns of the specimens regarding Species and Locality (Table 3).

224   *Alicornops simorrense* and *P. mirallesi* cluster together with higher anisotropy than *P. douvillei*, *B.*

225   *brachypus*, *B. gajense*, *M. welcommi*, *D. steinheimensis*, *H. tetradactylum*, and *L. sansaniense* (Table

9

226   3; p-value < 0.05). Concerning complexity, *B. gajense* and *H. tetradactylum* stood out for having

227   higher complexities compared to all other species besides *M. welcommi* and *G.* cf. *browni*. Moreover,

228   *G.* cf. *browni* was different from *B. brachypus*, both *Plesiaceratherium* species, and both

229   *Hispanotherium* species regarding complexity and HAsfc81 (Table 3). For both DMTA parameters in

230   which Locality had a noticeable effect (epLsar and Asfc), we found a cluster between Béon 1 and

231   Gračanica opposed to one containing at least Simorre and Sansan (for Asfc: also Kumbi 4 and

232   Villefranche d'Astarac; Table 3).

233   **Table 2: Pairs (Species or Locality) with noticeable p-values after Tukey's honestly significant**

234   **difference (HSD) by DMTA parameters.**

235   FTfv not precised as it yielded p-values above 0.1 only

236

DMTA parameter	Pair (Species or Locality) with differences		p-value
Anisotropy			
	Plesiaceratherium mirallesi	*Brachypotherium brachypus*	0.066
		Lartetotherium sansaniense	0.054
		Hoploaceratherium tetradactylum	0.09
Complexity			
	Hoploaceratherium tetradactylum	*Hispanotherium beonense*	0.008
		Prosantorhinus douvillei	0.01
		Plesiaceratherium mirallesi	6.3×10^{-4}
		Plesiaceratherium balkanicum	0.051
	Gračanica	Sansan	0.047
		Simorre	0.028
		Villefranche d'Astarac	0.032
HAsfc9			
	Hoploaceratherium tetradactylum	*Plesiaceratherium balkanicum*	0.059
		Plesiaceratherium mirallesi	0.024
HAsfc81			
	Hoploaceratherium tetradactylum	*Plesiaceratherium balkanicum*	0.096
		Plesiaceratherium mirallesi	0.072

237

Table 3: Fischer's least significant difference (LSD) post hoc results by DMTA parameters

239 Groups (a, ab, abc, b, bc, and c) are indicated with a p-value threshold of 0.05, for the sake of clarity.
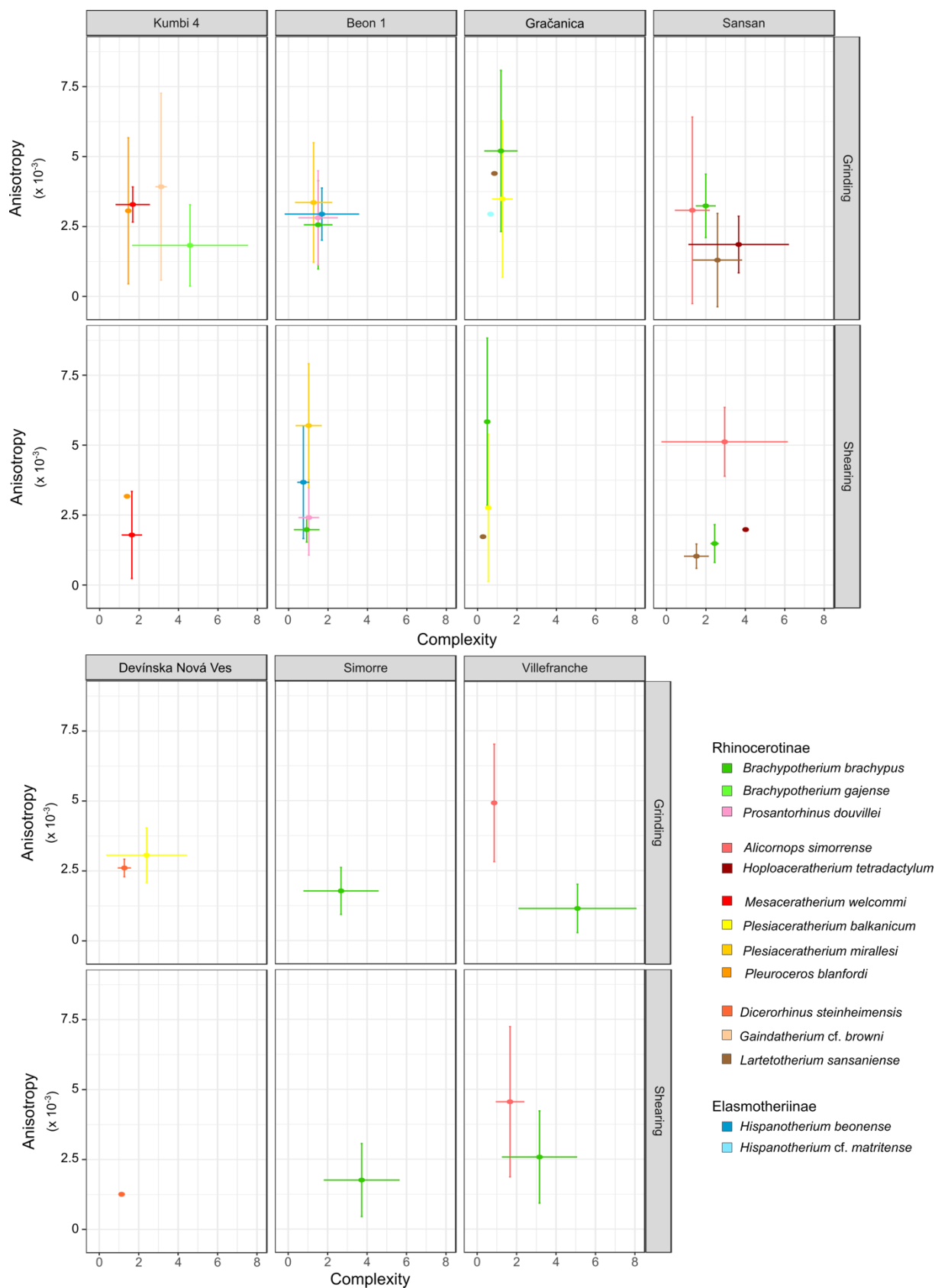
		a	ab	abc	b	bc	c
epLsar	**Species**	*A. simorrense* *P. mirallesi*	*G.* cf. *browni* *H. beonense* *H.* cf. *matritense* *P. balkanicum* *P. blanfordi*	-	*P. douvillei* *B. brachypus* *B. gajense* *M. welcommi* *D. steinheimensis* *L. sansaniense* *H. tetradactylum*	-	-
	Locality	Gračanica Béon 1	Villefranche d'Astarac Devínska Nová Ves Kumbi 4	-	Sansan Simorre	-	-
Asfc	**Species**	*B. gajense* *H. tetradactylum*	*G.* cf. *browni*	*M. welcommi*	-	*B. brachypus* *P. blanfordi* *A. simorrense* *D. steinheimensis* *L. sansaniense*	*P. douvillei* *P. balkanicum* *P. mirallesi* *H. beonense* *H.* cf. *matritense*
	Locality	Simorre Sansan Kumbi 4 Villefranche d'Astarac	Devínska Nová Ves	-	-	Béon 1	Gračanica
FTfv	**Species**	*H.* cf. *matritense* *B. gajense*	*P. blanfordi* *M. welcommi* *G.* cf. *browni* *D. steinheimensis* *H. tetradactylum* *P. douvillei* *H. beonense*	-	*B. brachypus* *A. simorrense* *P. balkanicum* *P. mirallesi* *L. sansaniense*	-	-
HAsfc9	**Species**	*G.* cf. *browni* *L. sansaniense* *H. tetradactylum*	*P. blanfordi* *B. gajense* *B. brachypus* *P. douvillei* *M. welcommi* *A. simorrense* *D. steinheimensis* *H. beonense*	-	*P. balkanicum* *P. mirallesi* *H.* cf. *matritense*	-	-
HAsfc81	**Species**	*G.* cf. *browni*	*B. gajense* *H. tetradactylum* *L. sansaniense*	*P. blanfordi* *P. douvillei* *M. welcommi* *A. simorrense* *D. steinheimensis*	-	*B. brachypus* *H. beonense*	*P. balkanicum* *P. mirallesi* *H.* cf. *matritense*

240

241   Besides at Béon 1, the microwear sampling was very restricted (n < 5), either due to low numbers of

242   exploitable teeth available, or to the lack of well-preserved microwear texture on molars. In order to

243   facilitate the understanding, the results are presented by locality (chronologically) and by species. At

244   **Kumbi 4**, four species were considered for DMTA: *Pleuroceros blanfordi*, *Mesaceratherium welcommi*,

245   *Gaindatherium* cf. *browni* (grinding only), and *Brachypotherium gajense* (grinding only). Figure 3

246   shows that Kumbi rhinocerotids display a great variety of microwear patterns. Only one specimen,

247   belonging to *G.* cf. *browni*, is above the high anisotropy threshold of 5 x 10^{-3}, while all specimens of *B.*

248   *gajense* and *G.* cf. *browni* but none of *P. blanfordi* display values above the high complexity cutpoint of

249   2. *Gaindatherium* cf. *browni* and *P. blanfordi* have large variations in anisotropy, from low values (~ 1 x

250   10^{-3}) to high (about 5 x 10^{-3}), but consistent values of complexity (around 3 and 1.4 respectively). Such

251   a pattern associated with moderate (*P. blanfordi*) to high (*G.* cf. *browsi*) values of HAsfc (Figure 4)

252   point towards mixed-feeding diets, probably with the inclusion of harder objects for *G.* cf. *browsi*. The

253   signature for *B. gajense* is suggestive of browsing with low mean anisotropy (1.82 x 10^{-3}), but high

254   means of complexity (4.58), FTfv (7.89 x10^{4}), and HAsfc (HAsfc9 = 0.36; HAsfc81 = 1). Eventually, *M.*

255   *welcommi* presents low to moderate anisotropy values (< 4 x 10^{-3}), a moderate complexity (~ 1.5) and

256   HAsfc, but high FTfv (> 4 x 10^{4}) on both facets (Figure 4), which denotes browsing or mixed-feeding

257   habits.

258

259   At **Béon 1**, the DMT of the four rhinocerotids overlap contrary to that of Kumbi 4 rhinocerotids (Figure

260   3). The DMTA results are already detailed in Hullot et al. (2021). They suggest a mixed-feeding

261   behavior for *H. beonense* with moderate anisotropy values (mostly < 4 x 10^{-3}), variable values of

262   complexity (low-medium), moderate-high FTfv (around 4 x 10^{4}), and moderate HAsfc on both facets

263   (Figure 4). *Plesiaceratherium mirallesi* is considered as a folivore due to low complexity (~ 1) and

264   HAsfc values but relatively high anisotropy (above 5 x 10^{-3}), indicating an abrasive but not diversified

265   diet. Concerning the teleoceratines, they display similar microwear textures (Figure 3; Figure 4),

266   though *B. brachypus* has lower values of anisotropy (< 2 x 10^{-3}). This suggests that *B. brachypus* was

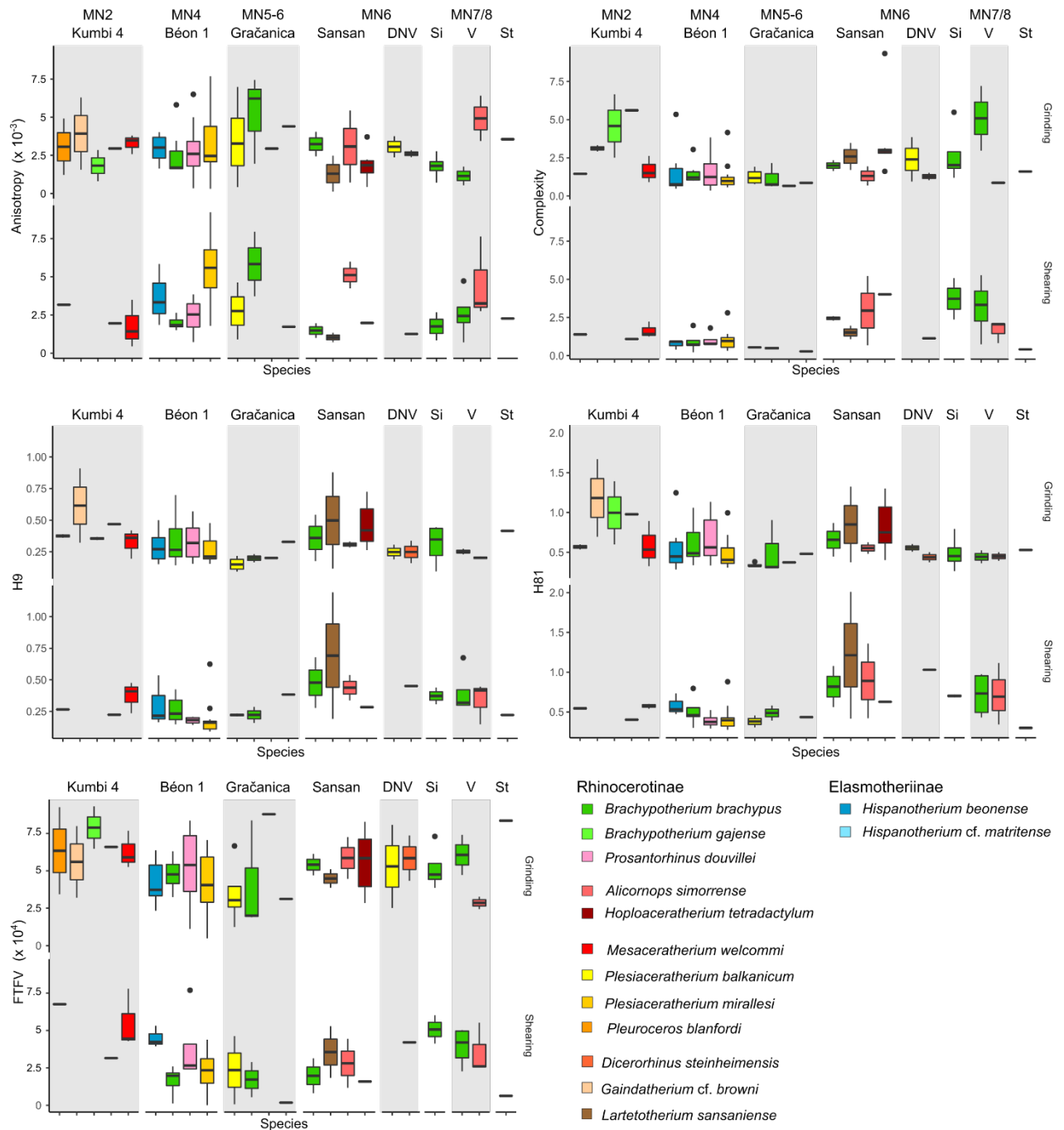267   probably a browser or a mixed-feeder, while *Pr. douvillei* was a browser favoring leaves.

Figure 3: Dental microwear results of early and middle Miocene rhinocerotids plotted as mean and standard deviation of anisotropy against that of complexity by facet, locality and species

271   Localities organized chronologically. Steinheim am Albuch not shown as only one specimen was

272   studied. Color code by species as indicated in the figure.

273

274

Figure 4: Dental microwear results of early and middle Miocene rhinocerotids plotted as

boxplots of each DMTA parameter by facet and species.

277   Time flows from left to right. DNV: Devínska Nová Ves, St: Steinheim am Albuch, Si: Simorre, V:

278   Villefranche d'Astarac. Color code by species as indicated in the figure and consistent with Figure 3.

14

279   At **Gračanica**, we also observe a great overlapping in the DMT. The complexity is very low for all

280   rhinocerotids studied (mostly below 1) suggesting soft food items. Anisotropy varies greatly but

281   HAsfc81 is consistently low (< 0.5) for all species (Figure 4). This points towards soft browsing or

282   folivory for all rhinocerotids at Gračanica.

283

284   At **Sansan**, the DMTA signatures of the rhinocerotids are more diversified and less overlapping,

285   similarly to Kumbi 4 (Figure 3). *Lartetotherium sansaniense* and *H. tetradactylum* have low values of

286   anisotropy (< 2.5 x 10^{-3}) and moderate (1-2; *L. sansaniense*) to high (> 2; *H. tetradactylum*) values of

287   complexity, recalling browsers. The high values of HAsfc (Figure 4) for both species are compatible

288   with a browsing diet. The other two species, *B. brachypus* and *A. simorrense*, are in the range of

289   mixed-feeders (Figure 3), and have compatible moderate to high values of HAsfc.

290

291   At **Devínska Nová Ves**, our restricted sample suggest browsing habits for both species *P. balkanicum*

292   and *D. steinheimensis*, with moderate values of both anisotropy (~ 2.5 x 10^{-3}) and complexity (mostly

293   between 1 and 1.5). FTfv is high on both facets (> 4 x 10^4) and HAsfc moderate (Figure 3; Figure 4).

294

295   At **Simorre**, *B. brachypus* specimens display low values of anisotropy (< 2.5 x 10^{-3} except two

296   specimens), and high values of complexity (> 2) and FTfv (> 4 x 10^4) on both facets. Values of HAsfc9

297   are high (> 0.3) on both facets, while that of HAsfc81 are moderate on the grinding facet (median =

298   0.45) and high on the shearing one (median = 0.7). These DMTA results suggest browsing

299   preferences with the inclusion of hard objects, probably fruits.

300

301   At **Villefranche d'Astarac**, *B. brachypus* and *A. simorrense* present well-distinguished DMT (Figure

302   3). *Brachypotherium brachypus* has low anisotropy values (< 2.5 x 10^{-3}) and high complexity ones (>

303   2.5) corresponding to a browsing signal, while the opposite is true for *A. simorrense*. The moderate

304   values of HAsfc for *A. simorrense* suggest that folivory is more likely than mixed-feeding for these

305   specimens and the corresponding individuals.

306

307   Eventually the specimen of *A. simorrense* from **Steinheim am Albuch** has a moderate anisotropy

308   (Grinding: 3.56 x 10^{-3}; Shearing: 2.27 x 10^{-3}), low (Shearing: 0.41) to moderate (Gringing: 1.6)

15

309   complexity, a high FTfv on the grinding facet (8.35×10^4) but low on the shearing one (0.63×10^4), and

310   low HAsfc on the shearing facet but moderate-high on the grinding one (Figure 4). This pattern is

311   consistent with browsing or mixed-feeding habits.

312

313   **GLMM**: For all response variables (epLsar, Asfc, FTfv, HAsfc9, and HAsfc81), model support

314   increased (i.e., lower AIC) when intraspecific factors (e.g., Facet, Genus, Locality) were included. The

315   final models contained three to seven factors, including Specimen, the random factor, by default in all

316   models. Facet was in the final models of epLsar and FTfv, Locality and Age were found in the final

317   models of Asfc and both HAsfc. Details and comparison of all models can be seen in electronic

318   supplementary material S5 and S6. Differences by Locality were also observed. Béon 1 had a lower

319   complexity than Kumbi 4, Sansan, Simorre, and Villefranche (df = 119, α = 0.05, |t-values| > 1.7),

320   while Tukey's contrasts highlighted lower values of Asfc for Gračanica than for Kumbi (p-value <

321   0.004), Simorre (p-value = 0.027), and Villefranche (p-value < 0.001). Moreover, Béon 1 had lower

322   HAsfc9 and HAsfc81 values than Kumbi 4 and Sansan (df = 119, α = 0.05, |t-values| > 1.7). Tukey's

323   contrasts also showed that Sansan had higher HAsfc9 and HAsfc81 than Gračanica (p-value ≤ 0.001).

324   The sampling site (tooth locus, position, side) had sometimes a confounding effect. For instance, M2

325   had higher epLsar values than M3 (df = 119, α = 0.05, t-value = -1.95).

326

327   **GLMM - Comparison to extant dataset**: When compared to the extant dataset (see S8 for all

328   details), we noticed that all fossil species had lower anisotropy values than the extant grazer

329   *Ceratotherium simum* (white rhinoceros) and the folivore *Dicerorhinus sumatrensis* (Sumatran

330   rhinoceros), although the classic t-value threshold was not reached for a few species (*P. blanfordi*, *G.

331   cf. browsi*, *B. gajense* [only regarding *C. simum*], *P. mirallesi*, and *A. simorrense*; α = 0.95, |t-values| ≤

332   1.7). On the contrary, *P. mirallesi* displayed higher values of anisotropy than the extant browsers

333   *Diceros bicornis* (black rhinoceros; t-value = 1.93) and *Rhinoceros sondaicus* (Javan rhinoceros; t-

334   value = 2.66). Regarding complexity, *C. simum* and *D. sumatrensis* had lower values than *B. gajense*

335   and *H. tetradactylum*, while the extant browsers had higher values than *P. balkanicum*, *P. douvillei*, *P.

336   mirallesi*, and *H. beonense* (α = 0.95, |t-values| > 1.7). All other DMTA parameters showed less

337   differences between the extant and fossil datasets: *C. simum* and *R. sondaicus* had higher FTfv,

338   HAsfc9, and HAsfc81 than *B. brachypus*, *P. balkanicum*, and *P. mirallesi* (α = 0.95, |t-values| > 1.7).
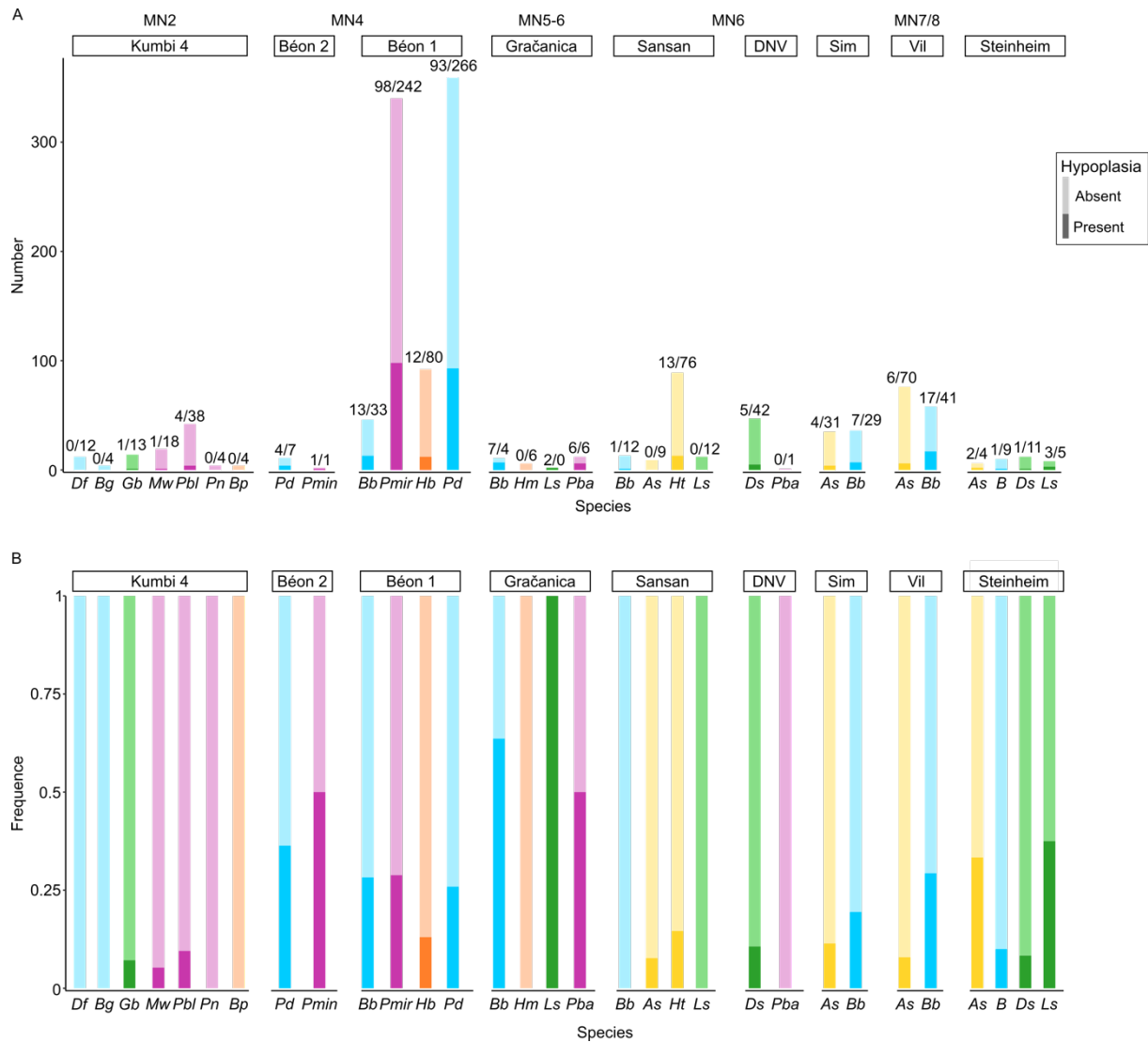
16

339   <u>Hypoplasia</u>

340   The overall prevalence of hypoplasia on rhinocerotid teeth from the early and middle Miocene

341   localities studied is high, with 302 teeth affected out of 1401, corresponding to over 20 % (21.56 %).

342   There are, however, marked discrepancies between species, localities, and tooth loci (Figure 5). The

343   most affected genera were *Plesiaceratherium* (104/357; 29.13 %), *Prosantorhinus* (97/370; 26.22 %),

344   and *Brachypotherium* (46/178; 25.84 %), but this resulted mostly from the dominance of Béon 1

345   specimens in our sample. *Brachypotherium brachypus* was often one of the most affected species at

346   all sites where the species was found, except Sansan (1/13; 7.69 %), contrary to *A. simorrense* often

347   found associated with the latter species and relatively spared by hypoplasia (maximum 4/35 = 11.43 %

348   of teeth affected at Simorre; Figure 6).

349

350   The prevalence was above 10 % for all localities except Kumbi 4, for which the overall prevalence is

351   low (6/99; 6.06 %; Table 4). Hypoplasia defects are quite rare at Kumbi 4 for all species studied, and

352   even null for the teleoceratine species (*D. fatehjangense* and *B. gajense*), *Bugtirhinus praecursor*, and

353   *Plesiaceratherium naricum* (Figure 6). Only *Pleuroceros blanfordi* appears a little more affected (4/42;

354   9.52 %), totaling four of the six hypoplasias observed at the locality. Hypoplasia was also relatively

355   limited at Sansan (14/132; 10.61 %) and Devínska Nová Ves (5/48; 10.42 %), with only *B. brachypus*

356   and *H. tetradactylum* affected at Sansan, and *D. steinheimensis* from the latter (Table 4 ; Figure 6). On

357   the contrary, the rhinocerotids from Béon 1, Béon 2, and Gračanica are very affected, with more than

358   25 % of the teeth presenting at least one hypoplasia at Béon 1 (216/832; 25.96 %) and Béon 2 (5/18;

359   27.78 %), and nearly 50 % at Gračanica (15/31; 48.39 %; Table 4). At these sites, the prevalence of

360   hypoplasia is high for all species but the elasmotheriines (Figure 6). Indeed, the elasmotheriines of all

361   sites were relatively spared (*H. beonense* at Béon 1: 13.04 %) or even not affected by hypoplasia (*B.*

362   *praecursor* at Kumbi 4 and *H.* cf. *matritense* at Gračanica).

363

Figure 5: Number (A) and Frequence (B) of hypoplasia by Locality and Species

Numbers on barplot A indicate the number of hypoplastic teeth (dark colors) versus unaffected ones (light colors). Frequencies are calculated as the ratio of hypoplastic teeth on the total number of teeth (hypoplastic and normal). Sub-tribes colored in blue: Teleoceratina, in green: Rhinocerotina; in yellow: Aceratheriina, in pink: stem Rhinocerotinae, and in orange: Elasmotheriina

Abbreviations: DNV: Devínska Nová Ves, Sim: Simorre, Vil: Villefranche d'Astarac

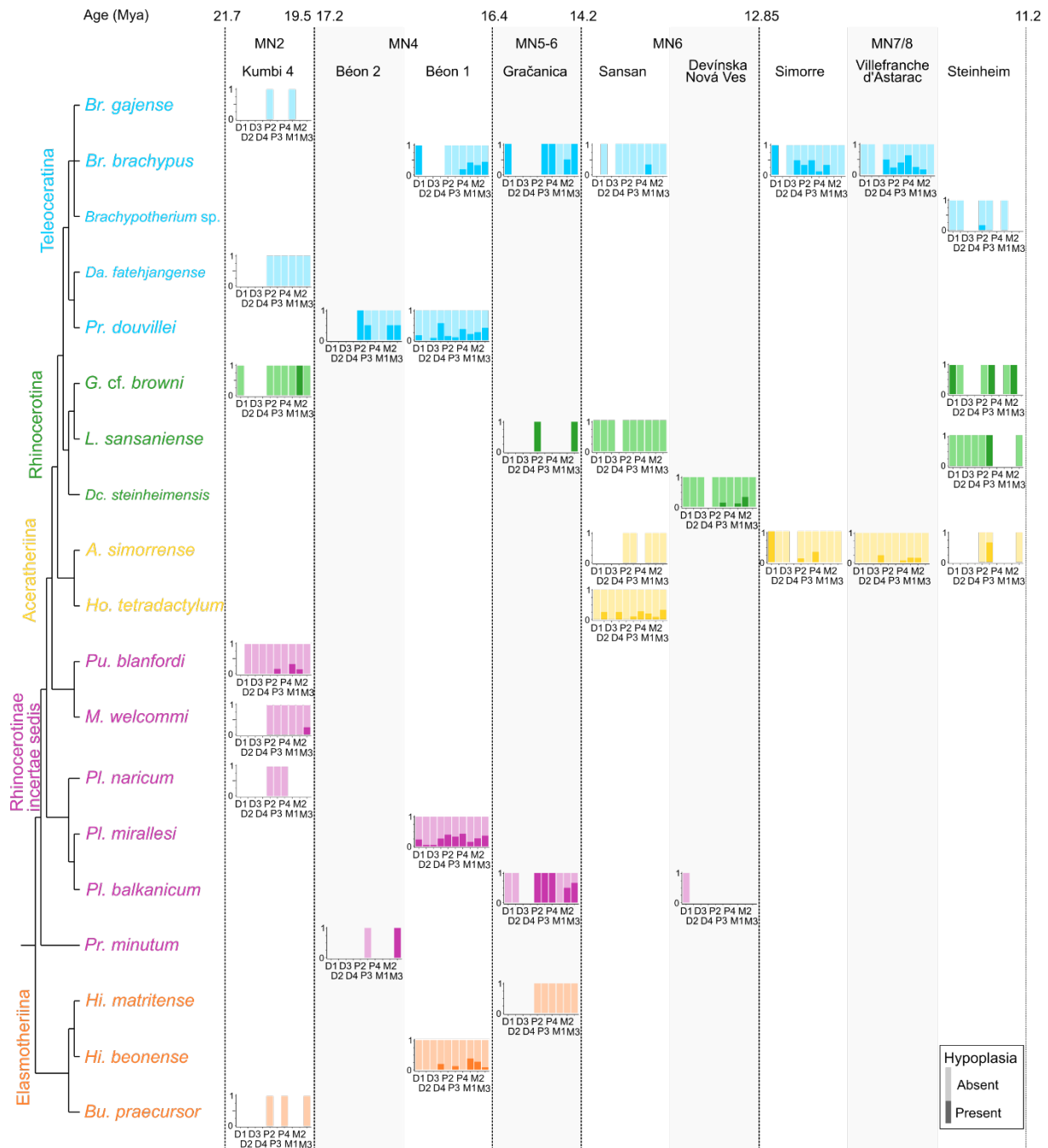*Df*: *Diaceratherium fatehjangense*, *Bg*: *Brachypotherium gajense*, *Bp*: *Bugtirhinus praecursor*, *Gb*: *Gaindatherium* cf. *browni*, *Mw*: *Mesaceratherium welcommi*, *Pbl*: *Pleuroceros blanfordi*, *Pn*: *Plesiaceratherium naricum*, *Pmin*: *Protaceratherium minutum*, *Pd*: *Prosantorhinus douvillei* (*P.* aff. *douvillei* at Béon 2), *Bb*: *Brachypotherium brachypus*, *Hb*: *Hispanotherium beonense*, *Pmir*: *Plesiaceratherium mirallesi*, *Hm*: *Hispanotherium* cf. *matritense*, *Ls*: *Lartetotherium sansaniense*, *Pba*:

18

Plesiaceratherium balkanicum, *As*: *Alicornops simorrense*, *Ht*: *Hoploaceratherium tetradactylum*, *Ds*:

Dicerorhinus steinheimensis, *B*: *Brachypotherium* sp.

Figure 6: Prevalence of hypoplasia by locality, species and tooth locus plotted against

phylogeny

Phylogenetic relationships follow formal parsimony analyses (Antoine, 2002; Antoine et al., 2010;

Becker et al., 2013; Tissier et al., 2020).

19

384   Subtribes colored in blue: Teleoceratina, in green: Rhinocerotina; in yellow: Aceratheriina, in pink:

385   stem Rhinocerotinae, and in orange: Elasmotheriina

386   Dark colors: hypoplastic teeth; Light colors: unaffected teeth

387

388   **Table 4: Prevalence of hypoplasia by locality (number of specimens/percentages)**

	Hypoplastic	Normal	Percentage of hypoplasia
Kumbi 4	93	6	6.06
Béon 2	13	5	27.78
Béon 1	616	216	25.96
Gračanica	16	15	48.39
Devínska Nová Ves	43	5	10.42
Sansan	118	14	10.61
Simorre	60	11	15.49
Villefranche d'Astarac	111	23	17.16
Steinheim	29	7	19.44

389

390

391   Concerning the loci, milk teeth (47/294; 15.99 %) were overall less affected by hypoplasia than

392   permanent ones (255/1107; 23.04 %; Table 5). Indeed, besides at Béon 1, very few milk molars are

393   hypoplastic (one D1/d1 at Gračanica and Steinheim, two D1 at Simorre, two D2 and 1 d4 at Sansan, 4

394   D4/d4 at Villefranche d'Astarac). Upper and lower teeth were equally affected (Kruskal-Wallis, df = 1,

395   p-value = 0.11), with respectively 19.86 % (144/725) and 23.37 % (158/676) of teeth bearing

396   hypoplasia. The most affected locus was the fourth milk molar with 38.24 % (26/68), while the least

397   affected were second and third milk molars with around 4 % affected (3/68 and 3/72 respectively;

398   Table 5). Other loci particularly affected were fourth premolars (60/200; 30 %), third molars (50/188;

399   26.60 %), and second molars (49/202; 24.26 %; Table 5). Once again, these findings mostly result

400   from the dominance of Béon 1 specimens in the sample, and great differences in the hypoplasia

401   pattern are observed by locality (Figure 6). Indeed, if virtually all tooth loci are likely to be affected for

402   Béon 1 rhinocerotids, the pattern is less varied at other localities although it seemingly diversifies with

403   sample size (e.g., *H. tetradactylum* from Sansan and Villefranche d'Astarac). For instance, hypoplastic

404   teeth are nearly exclusively molars at Kumbi 4 (with only one defect on a p3), and permanent teeth at

405   Gračanica (only one defect on a D1; Figure 6).

406

407 **Table 5: Prevalence of hypoplasia by tooth locus, regardless of provenance and taxon**

408 Upper and lower teeth merged as they have a similar timing of development

	Hypoplastic	Normal	Percentage of hypoplasia
D1	71	15	17.44
D2	65	3	4.41
D3	69	3	4.17
D4	42	26	38.24
Total decidual teeth	47	247	15.99
P2	130	26	16.67
P3	138	33	19.30
P4	140	60	30.00
M1	153	37	19.47
M2	153	49	24.26
M3	138	50	26.60
Total permanent teeth	255	852	23.04

409

410 **GLMM**: For all response variables (Hypo, Defect, Multiple, Localization, and Severity), model support

411 increased (i.e., lower AIC) when intraspecific factors (e.g., Tooth Loci, Genus, Locality) were included.

412 When Genus was not forced into the models, the final models contained three to six factors, including

413 Specimen, the random factor, by default in all models. Defect (converted to a factor) was in the final

414 models of all concerned variables (Multiple, Localization, and Severity). Genus was in the final models

415 of all variables but Localization. Position was in the final models of Hypo, Defect, and Localization,

416 while Tooth, and Wear were in that of Hypo and Defect. Details and comparison of all models can be

417 seen in electronic supplementary material S5 and S7.

418

419 Based on GLMMs results, we can assess the influence of Genus, Locality, and Tooth on the

420 hypoplasia pattern. *Alicornops* was less affected than *Brachypotherium* (p-value = 0.015), while

421 *Plesiaceratherium* was more prone to hypoplasia than *Hispanotherium* (p-value = 0.02). GLMMs

422 revealed differences in the patterns of hypoplasia (i.e., type of defects and their frequencies) between

423 *Brachypotherium* and the following taxa: *Dicerorhinus* (p-value = 0.0046), *Alicornops* (p-value <

424 0.001), and *Protaceratherium* (p-value = 0.034). Tukey's contrasts also revealed the lowest p-values

425 between *Alicornops* and the following taxa: *Hispanotherium* (p-value = 0.064), *Plesiaceratherium* (p-

426 value < 0.01), *Prosantorhinus* (p-value < 0.01), *Protaceratherium* (p-value = 0.05). Eventually

427   *Dicerorhinus* had a different hypoplasia pattern than *Plesiaceratherium* (p-value = 0.034) and

428   *Prosantorhinus* (p-value = 0.071).

429

430   Concerning tooth loci, all teeth but fourth premolars and third molars are less affected than fourth milk

431   molars (p-values < 0.05). The results further suggested that the most commonly affected loci were

432   third molars, fourth premolars and fourth milk molars, while the least affected were all milk molars but

433   the fourth. Concerning localities, Gračanica teeth were significantly more touched than Béon 1 and

434   Sansan specimens (p-values ≈ 0.01). Middle Miocene rhinocerotids present a hypoplasia pattern

435   distinct from that of early Miocene ones (p-value = 0.019). Similarly to GLMMs for DMTA, we observed

436   confounding effects. Slightly-worn teeth had less hypoplasia than average worn (p-value = 0.005) and

437   very worn teeth (p-value = 0.026).

438

439   **Discussion**

440

441   <u>Dietary preferences and niche partitioning of the rhinocerotids studied</u>

442   The comparison of the fossil specimens DMT to that of extant ones highlighted important differences.

443   This suggests that the dietary spectrum of extinct rhinocerotids might have been very distinct from that

444   observed in the living species (Hullot et al., 2019). However, the microwear textures of the fossils are

445   critically distinct from that of the only extant strict grazer *Ceratotherium simum*, banning such dietary

446   preferences for the studied fossil specimens. This finding is not surprising as grasses and associated

447   grazing ungulates expended only during latest Miocene in Eurasia (Janis, 2008). The reconstructed

448   dietary preferences based on DMTA are presented in Table 6 by locality and by species.

449

450   The DMTA results of fossil specimens on both facets (Figure 3; Figure 4) suggest a clear niche

451   partitioning based on feeding preferences for the rhinocerotid specimens studied at Kumbi 4, Sansan,

452   and Villefranche d'Astarac. Although DMT could only be explored in four out of the nine rhinocerotid

453   species present at Kumbi 4, the patterns observed indicate clear differences in the feeding behaviors,

454   even if leaf consumption seems to be a major component for all rhinocerotids studied but *B. gajense*.

455

Table 6: Dietary preferences inferred from textural microwear (DMTA) of the studied rhinocerotid specimens from different fossil localities of the lower and middle Miocene of Eurasia.

Color code: brown/B – browser, blue/M – mixed-feeder, light green/F – folivore, no color/x – not studied

	Kumbi 4	Béon 2	Béon 1	Gračanica	Sansan	Devínska Nová Ves Spalte	Simorre	Villefranche d' Astarac	Steinheim am Albuch
Rhinocerotinae									
Mesaceratherium welcommi	M								
Pleuroceros blanfordi	M								
Protaceratherium sp.	x								
Protaceratherium minutum		x							
Plesiaceratherium naricum	x								
Plesiaceratherium mirallesi		x	F						
Plesiaceratherium balkanicum				F		B			
Plesiaceratherium sp.									
Hoploaceratherium tetradactylum					B				
Alicornops simorrense					M		x	F	M
Gaindatherium cf. *browni*	M								
Lartetotherium sansaniense				B	B				x
Dicerorhinus steinheimensis						B			x
Diaceratherium fatehjangense	x								
Brachypotherium gajense	B								
Brachypotherium brachypus				M	F	M	B	B	
Brachypotherium sp.									x
Prosantorhinus shahbazi	x								
Prosantorhinus douvillei			aff. B						
Elasmotheriinae									
Bugtirhinus praecursor	x								
Hispanotherium beonense			M						
Hispanotherium cf. *matritense*				M					

This finding is in line with the inferred lush vegetation under warm and moist climatic conditions proposed for this locality (Antoine et al., 2010, 2013; Martin et al., 2011). The dietary preferences reconstructed for Sansan rhinocerotids suggest the co-occurrence of two browsers (*L. sansaniense* and *H. tetradactylum*, the latter including harder items in its diet) and two mixed-feeders (*A. simorrense* and *B. brachypus*), coherent with the (sub-)tropical forested environment reconstructed for that locality (Costeur et al., 2012), but at odds with the recent-like Miocene coolhouse as depicted by Westerhold et al. (2020; ~415 parts per million CO_2). This niche partitioning is probably accentuated by different habitat preferences: *H. tetradactylum* is mostly found in swamp or fluvial sediments

23

472   indicating wet habitat preferences contrary to *A. simorrense*, while *B. brachypus* seems intermediate

473   and *L. sansaniense* generalist (Heissig, 2012). Eventually, we observed obvious differences in the

474   dietary preferences for *A. simorrense* (folivore or mixed-feeder favoring leaves) and *B. brachypus*

475   (browser including hard objects) at Villefranche d'Astarac, where a humid forested environment is

476   hypothesized (Bentaleb et al., 2006).

477

478   On the contrary, an overlap of microwear textures, especially for the grinding facet, is observed for the

479   localities of Béon 1 and Gračanica. Besides diet, different habitats and feeding heights might result in

480   niche partitioning (Hutchinson, 1959; Arsenault and Owen-Smith, 2008). Concerning Béon 1, a partial

481   niche partitioning due to habitat differences has been hypothesized for the rhinocerotids – swamps for

482   both teleoceratines *B. brachypus* and *P. douvillei*, open woodland for *P. mirallesi*, and savannah-like

483   open environments for *H. beonense* (Bentaleb et al., 2006) – and subtle dietary differences are

484   discussed in Hullot et al. (2021) in the light of the combination of molar mesowear and dental

485   microwear texture analysis. At Gračanica, 2D microwear and mesowear score already revealed an

486   overlap in the dietary preferences of *Pl. balkanicum* and *B. brachypus* as two browsing species,

487   although the latter is labelled as "dirty browsing", a dietary category (not defined by comparative

488   datasets on intensively studied extant species with known diets) including species assumed to browse

489   and incorporate soil particles. (Xafis et al., 2020). Although microwear sampling is restricted and

490   includes premolars for the other two rhinocerotids (*L. sansaniense* and *H.* cf. *matritense*), it points

491   towards different mixed-feeding behaviors, most likely with a dominance of grass in the diet of *H.* cf.

492   *matritense* (Xafis et al., 2020). The very low values of complexity for all Gračanica rhinocerotids in our

493   sample, combined to relatively high values of anisotropy (Figure 3; Figure 4), could suggest an

494   important consumption of leaves for all species, as well as a very low amount of lignified tissues that

495   would have required more grinding to get access to cell content. Interestingly, the reconstructed

496   environment at this locality (based on mammal assemblage and flora) is a lowland swamp surrounded

497   by a closed canopy-like environment (Butzmann et al., 2020; Xafis et al., 2020), meaning that leaves

498   would have been an abundant resource. This recalls the feeding preferences and microwear textures

499   of the extant *Dicerorhinus sumatrensis* (Sumatran rhino; Hullot et al., 2019). Eventually, the restricted

500   DMTA samples from Devínska Nová Ves Spalte, Steinheim am Albuch, and Simorre suggest browsing

24

501   or mixed-feeding habits for all specimens studied, but did not allow to conclude on potential

502   competition for food resources.

503

504   <u>Interactions with co-occurring herbivores</u>

505   Besides other rhinocerotid species, the individuals studied co-occurred with many other herbivore

506   mammals. Although co-occurrence is not necessarily a good proxy for ecological interactions

507   (Blanchet et al., 2020), it is possible that some of these herbivores were competing for or partitioning

508   food resources with the rhinocerotids. Unfortunately, very little has been studied concerning the dietary

509   preferences of the fauna at most of the studied localities with the notable exceptions of Gračanica and

510   Sansan.

511

512   Indeed, recent studies on dental wear (micro- and meso- wear) or stable isotopy, suggested frugivory

513   for some associated species such as tragulids (*Dorcatherium* spp. at all localities but Simorre and

514   Villefranche; Aiglstorfer et al., 2014; Xafis et al., 2020), the middle Miocene Moschidae (*Micromeryx*

515   spp. found at Sansan, Simorre and Steinheim am Albuch; Aiglstorfer and Semprebon, 2019) or the

516   chalicothere *Metaschizotherium fraasi* (found at Steinheim am Albuch; Semprebon et al., 2011).

517   Interestingly, no rhinocerotid specimens studied here seemingly favored fruits. Similarly, the lophodont

518   suid *Listriodon splendens*, found at Gračanica, Devínska Nová Ves, and Simorre, might have favored

519   grasses (Van der Made, 2003; Xafis et al., 2020), a resource not exploited by the rhinocerotids either.

520   Otherwise, the vast majority of herbivore species were probably browsers or mixed-feeders, in good

521   agreement with the statement by Eronen and Rössner (2007) that these forms were dominant

522   between MN4 and MN9. This is for instance the case of the associated perissodactyl species

523   *Anisodon grande* (Chalicotheriidae), which 2D microwear signal at Devínska Nová Ves suggests

524   folivory (Semprebon et al., 2011), and *Anchitherium* spp. (Equidae) ranging from generalists to "dirty

525   browsers" (Kaiser, 2009; Xafis et al., 2020).

526

527   Within browsers and mixed-feeders, resources partitioning is still possible (e.g., consumption of

528   different plant parts or species) but might be difficult to detect in fossil communities. Moreover, other

529   strategies can lead to niche partitioning, such as different habitat, different body mass, or different

530   feeding height (Hutchinson, 1959; Schoener, 1974; Arsenault and Owen-Smith, 2008). Regarding

531   body mass, most rhinocerotids studied are megaherbivores *sensu* Owen-Smith (1988; terrestrial

25

532   herbivores weighting more than 1000 kg), which implies specific feeding strategies and metabolic

533   requirements. Megaherbivores are often treated as a separate herbivore guild, mostly disturbing that

534   of mesoherbivores (4–450 kg ; Fritz et al., 2002; Calandra et al., 2008; Landman et al., 2013). Within

535   megaherbivores, proboscideans frequently co-occurred with rhinocerotids at the studied localities and

536   were mostly browsers or mixed-feeders, placing them as direct competitors for rhinocerotids. Indeed,

537   the mesowear and 2D microwear suggest that *Prodeinotherium bavaricum* and *Gomphotherium*

538   *angustidens* were browsers at Gračanica (Xafis et al. 2020), while the mesowear angle categorizes *P.*

539   *bavaricum* from Sansan, *D. giganteum* from Villefranche d'Astarac and *G. angustidens* from Simorre

540   as browsers, but *G. angustidens* from Sansan and Villefranche d'Astarac as mixed-feeders (Loponen,

541   2020). Such overlapping in the diet of proboscideans and rhinocerotids is observed nowadays

542   between African elephants and black rhinoceroses (Landman et al., 2013). Interestingly, this

543   competition is detrimental to the rhinoceros, whose individuals shift towards the inclusion of more

544   grasses in presence of elephants (on a seasonal basis). Another possibility, as postulated by Xafis et

545   al. (2020) for *Deinotherium* spp. and *Plesiaceratherium balkanicum* at Gračanica, would be different

546   feeding heights between proboscideans and rhinocerotids, as the first ones were most likely feeding at

547   the top of trees due to their larger size (some of the biggest Neogene mammals; Larramendi, 2015).

548

549   Hypoplasia prevalence and environmental conditions

550   We found that the hypoplasia prevalence and pattern (i.e., tooth loci affected) were very different

551   depending on the locality and the species concerned. Except for Kumbi 4, the prevalence was

552   relatively high (> 10 %) at all sites of our early-middle Miocene sample. Even though nine species of

553   rhinocerotids are found at Kumbi 4, such a low prevalence is in agreement with previous results in the

554   region over the Cenozoic (Roohi et al., 2015), and coherent with the very favorable, low-stress context

555   hypothesized at this locality, that is a rich vegetation under a warm and humid climate (Antoine et al.,

556   2013).

557

558   The prevalence of hypoplasia is high at Béon 1 (>25 %) for all rhinocerotids except *H. beonense*, with

559   molars being particularly affected with respect to other dental loci. Second and third molars are the last

560   teeth to develop and erupt in rhinocerotids (Hitchins, 1978; Hillman-Smith et al., 1986; Böhmer et al.,

561   2016), and stresses on these late-developed teeth have been correlated with environmental, seasonal

562   stresses in sheep (Upex and Dobney, 2012). Although subtropical wet conditions are reconstructed at

563   Béon 1 (just prior to the MCO), periodic droughts are also reported in the area at that time (Duranthon

564   et al., 1999; Hullot and Antoine, 2020). Interestingly, the least affected species is the elasmotheriine *H.*

565   *beonense*, an early representative of a clade adapted to relatively open and arid environments

566   (Cerdeño and Nieto, 1995; Iñigo and Cerdeño, 1997), and which displays a mixed-feeding diet (Figure

567   4). On the contrary, both teleoceratine species, often considered swamp dwellers, display a high

568   prevalence of hypoplasia (Figure 5).

569

570   We found a very high prevalence of hypoplasia at Gračanica, with nearly 50 % of the teeth bearing at

571   least one hypoplastic defect. The proposed age for the locality ranges between 14.8 and 13.8 Ma

572   (Göhlich and Mandic, 2020), which is an interval of great climatic changes. Indeed, though included in

573   the MCO, the interval from 14.7 to 14.5 Ma present an increased seasonality in precipitations, with

574   prolonged dry periods (Böhme, 2003). On the other hand, an abrupt cooling occurred between 14 and

575   13.5 Ma, correlating with the Mi-3 event (Zachos et al., 2001; Böhme, 2003; Holbourn et al., 2014;

576   mMCT of Westerhold et al., 2020). Besides this challenging environmental context for the

577   rhinocerotids, our DMTA results suggest a potential competition for food resources (Figure 3), that

578   could have generated stressful conditions.

579

580   At Sansan, the prevalence of hypoplasia is overall moderate (~ 10 %) and defects are only found in

581   two species out of four: *H. tetradactylum* and *B. brachypus* (only one M1). The pattern of hypoplasia

582   for *H. tetradactylum*, with various loci affected, suggests different stresses and timing, from *in utero*

583   (D2) to post-weaning (M3). It is quite remarkable, as the proximity of the MCO peak (Maridet and Sen,

584   2012) leading to seasonal warm and moist conditions (Costeur et al., 2012), would seemingly

585   constitute relatively low stress conditions for the concerned rhinocerotids.

586

587   The prevalence of hypoplasia at Devínska Nová Ves Spalte is also moderate (5/48; 10.42 %) and

588   restricted to *D. steinheimensis* (P3, M1, M2 only; Figure 6), although the locality dates from the

589   mMCT. However, despite this transitional climatic system, pollen data from the Vienna Basin, to which

590   the locality belongs, indicate that regional conditions remained tropical with few precipitation variations

591   (Sabol and Kováč, 2006), coherent with the absence of hypoplasia on third molars, that can be

592   correlated with seasonal stresses. The paleogeographic context seems to have played a major role,

593   as the taxonomic differences with Sansan are partly explained by different paleoenvironments:

594   Devínska Nová Ves Spalte was a forested area near the shoreline of the transgressive late Langhian

595   sea (Sabol and Kováč, 2006).

596

597   The rhinocerotids from the localities of the MN7/8 (Simorre, Villefranche d'Astarac, and Steinheim am

598   Albuch), a time of sea-level drop and comparatively dry climate (Legendre et al., 2005; Böhme et al.,

599   2011; Heissig, 2012; Westerhold et al., 2020), present higher prevalences but contrasted patterns

600   depending on the species and locality (Figure 5; Figure 6). However, contrary to what we could have

601   been expected regarding the environmental conditions, the most affected loci (P2, P3, D1) document

602   mostly early-life stresses (e.g., birth, juvenile disease), rather than environmental or seasonal stresses

603   (Niven et al., 2004; Upex and Dobney, 2012). At Steinheim, only *L. sansaniense* has hypoplasia on

604   other teeth than second and third premolars, suggesting mostly early life stresses. At Simorre, more

605   loci are affected (D1, P2-P3, P4, and M1) and the pattern is relatively similar for both co-occurring

606   species i.e., *B. brachypus* and *A. simorrense*. Hypoplasia on D1, that develops mostly *in utero*

607   synchronously with D4, could indicate birth-related stresses (Hillman-Smith et al., 1986; Mead, 1999;

608   Böhmer et al., 2016). Similarly, the M1 starts its development relatively early, attested by the presence

609   of a neonatal line in some rhinocerotid teeth (Tafforeau et al., 2007), revealing particularly stressful

610   conditions around birth. Eventually, the rhinocerotids from Villefranche d'Astarac document later-life

611   stresses, with hypoplasia recorded from D4 to M2 (not P2-P3 for *A. simorrense*). The fourth premolars

612   are particularly affected in *B. brachypus*, which could indicate harsh weaning or cow-calf separation

613   conditions.

614

615   <u>Paleoecologic implications and changes</u>

616   Several species or genera are retrieved in various localities overtime, but *B. brachypus* clearly has the

617   longest range (from Béon 1 [MN4] to Simorre + Villefranche d'Astarac [MN7/8], with Gračanica [MN5-

618   6] and Sansan [MN6] in the meantime). We observe a clear shift in the DMT of *B. brachypus* over time

619   from a mixed-feeding behavior at Béon 1, Gračanica, and Sansan to a clear browsing signal with the

620   ingestion of harder items (fruits, seeds, or even soil) at Simorre and Villefranche d'Astarac (Figure 3;

621   Figure 4). This result could be due to a change in the regional climatic conditions, from warm and

622   humid pre-MCO to cooler, more seasonal and arid post-MCO (Zachos et al., 2001; Böhme, 2003;

623   Holbourn et al., 2014), perhaps leading to behavioral changes in this species (Cerdeño and Nieto,

624   1995), and/or to changes in local conditions.

625

626   Contrastingly, the DMT of *A. simorrense* remains quite similar from Sansan (MN6) to Steinheim

627   (MN7/8; Figure 3; Figure 4). Interestingly, there are clear differences in the hypoplasia prevalence of

628   these two species, *B. brachypus* being one of the most affected species in our sample. Such

629   differences in the hypoplasia prevalence could reveal the existence of a competition for food and/or

630   water resources. The pattern of hypoplasia at Simorre (D1, P2-P3) and Villefranche d'Astarac (D4-M1,

631   P4-M2) suggests early life stresses for both rhinocerotids (Figure 6), mostly before weaning (Mead,

632   1999).

633

634   Concerning other species found at more than one locality (*L. sansaniense*, *D. steinheimhensis*, and

635   *Plesiaceratherium* spp.), the hypoplasia patterns seem to be different at each locality, denoting a

636   greater effect of local conditions than species-related sensitivities. Only the *Plesiaceratherium* species

637   from Béon 1 and Gračanica exhibit comparable patterns (Figure 6), although it could be related to the

638   high prevalence of stresses for individuals belonging to the concerned taxa at these localities. Overall,

639   the elasmotheriines (*Bugtirhinus* and *Hispanotherium*) were seemingly spared by hypoplasia. Indeed,

640   no tooth was hypoplastic at Kumbi 4 (*B. praecursor*; 0/4) and Gračanica (*H.* cf. *matritense*; 0/6). At

641   Béon 1, for which a greater sample is available, *H. beonense* is the least affected species with 13.04

642   % (12/92) of hypoplastic teeth, nearly exclusively permanent (only one hypoplasia on a D4). If this

643   result was not surprising at Kumbi 4, where low-stress conditions were inferred and very little

644   hypoplasia recorded for all studied species, the difference to other associated species was particularly

645   striking at Béon 1 and Gračanica. The microwear study of elasmotheriines is restricted in the literature,

646   but it suggests the inclusion of a non-negligible part of browse resources in the diet, at least

647   seasonally (Rivals et al., 2020; Xafis et al., 2020). This finding is in line with our DMTA results for

648   *Hispanotherium* species (Béon 1 and Gračanica) suggesting mixed-feeding preferences (Figure 3;

649   Figure 4). The increasing crown height observed in this clade over time could allow for

650   accommodating to a greater variety of food items (Semprebon and Rivals, 2007; Damuth and Janis,

651   2011; Tütken et al., 2013), thus limiting nutritional stress, as observed in hipparionine equids, with

29

652   respect to anchitheriine equids (MacFadden, 1992; Janis, 2008; Mihlbachler et al., 2011). The classic

653   view of elasmotheriines as obligate open-environment rhinocerotids adapted to grazing – notably

654   based on representatives from the arid Iberic Peninsula (Iñigo and Cerdeño, 1997) – is thus somehow

655   challenged. This could mean that hypsodonty in this clade might counterbalance significant grit load

656   induced by feeding low in open environments, thus reflecting more the habitat rather than the diet, an

657   hypothesis that has already been proposed to explain hypsodonty evolution (Janis, 1988; Jardine et

658   al., 2012; Semprebon et al., 2019).

659

660   **Conclusions**

661

662   The study of the paleoecology of rhinocerotids from the early and middle Miocene of Eurasia revealed

663   clear differences over time and space between or within species. Though, DMTA results suggested

664   only browsers and mixed-feeders (no grazers nor frugivores) in the studied rhinocerotid sample, they

665   unraveled clear niche partitioning through food resources at several diachronous localities (Kumbi 4,

666   Sansan, and Villefranche d'Astarac). At other localities (Béon 1, Gračanica), a significant overlap of

667   microwear textures was observed, and more subtle differences in food preferences and other niche

668   partitioning strategies (habitat, feeding height) may have existed. Regarding enamel hypoplasia, which

669   is quite prevalent in the studied sample (except in the oldest and only South Asian locality, Kumbi 4), it

670   revealed clear disparities between localities, species, and dental loci. While the effects of climate

671   changes were not immediately obvious, we discussed more specific, local conditions that may explain

672   the observed stresses. Regarding a potential phylogenetic effect, we were able to highlight very

673   different sensitivities: while *B. brachypus* is highly affected by hypoplasia regardless of locality and

674   conditions, elasmotheriines (*Bugtirhinus praecursor* at Kumbi 4, *Hispanotherium beonense* at Béon 1

675   and *H.* cf. *matritense* at Gračanica) are pretty spared in contrast. Over time and depending on the

676   conditions, differences in DMT and/or prevalence of hypoplasia were observed for some species found

677   in several localities. This is notably the case for the feeding preferences of *B. brachypus*, oscillating

678   between browser and mixed feeder, or for the hypoplasia profiles of *L. sansaniense* and *D.*

679   *steinheimensis* denoting different stress periods and local conditions.

680

681

References

Aiglstorfer, M., and G. M. Semprebon. 2019. Hungry for fruit? – A case study on the ecology of middle Miocene Moschidae (Mammalia, Ruminantia). Geodiversitas, 41:385–399. doi: 10.5252/geodiversitas2019v41a10.

Aiglstorfer, M., G. E. Rössner, and M. Böhme. 2014. *Dorcatherium naui* and pecoran ruminants from the late Middle Miocene Gratkorn locality (Austria). Palaeobiodiversity and Palaeoenvironments, 94:83–123.

Antoine, P.-O. 2002. Phylogénie et évolution des Elasmotheriina (Mammalia, Rhinocerotidae). Mémoires Du Muséum National d'Histoire Naturelle, 188:5–350.

Antoine, P.-O. in press. Rhinocerotids from the Siwalik faunal sequence; p. *In* C. Badgley, D. Pilbeam, and M. Morgan (eds.), At the Foot of the Himalayas: Paleontology and Ecosystem Dynamics of the Siwalik Record of Pakistan., Johns Hopkins University Press.

Antoine, P.-O., and F. Duranthon. 1997. Découverte de *Protaceratherium minutum* (Mammalia, Rhinocerotidae) dans le gisement Orléanien (MN 4) de Montréal-du-Gers (Gers). Annales de Paléontologie (Vert.-Invert.), 83:201–213.

Antoine, P.-O., and J.-L. Welcomme. 2000. A New Rhinoceros From The Lower Miocene Of The Bugti Hills, Baluchistan, Pakistan: The Earliest Elasmotheriine. Palaeontology, 43:795–816. doi: 10.1111/1475-4983.00150.

Antoine, P.-O., and D. Becker. 2013. A brief review of Agenian rhinocerotids in Western Europe. Swiss Journal of Geosciences, 106:135–146. doi: 10.1007/s00015-013-0126-8.

Antoine, P.-O., F. Duranthon, and P. Tassy. 1997. L'apport des grands mammifères (Rhinocérotidés, Suoidés, Proboscidiens) à la connaissance des gisements du Miocène d'Aquitaine (France). BoiChro'M97, spécial 21:581–590.

Antoine, P.-O., K. F. Downing, J.-Y. Crochet, F. Duranthon, L. J. Flynn, L. Marivaux, G. Métais, A. R. Rajpar, and G. Roohi. 2010. A revision of *Aceratherium blanfordi* Lydekker, 1884 (Mammalia: Rhinocerotidae) from the Early Miocene of Pakistan: postcranials as a key. Zoological Journal of the Linnean Society, 160:139–194. doi: 10.1111/j.1096-3642.2009.00597.x.

Antoine, P.-O., G. Métais, M. Orliac, J. Crochet, L. Flynn, L. Marivaux, A. Rajpar, Dr. G. Roohi, and J. Welcomme. 2013. Mammalian Neogene biostratigraphy of the Sulaiman Province, Pakistan; p. 400–422. *In* Fossil Mammals of Asia: Neogene Biostratigraphy and Chronology. Columbia University Press doi: 10.13140/2.1.3584.5129.

Arman, S. D., T. A. A. Prowse, A. M. C. Couzens, P. S. Ungar, and G. J. Prideaux. 2019. Incorporating

722 intraspecific variation into dental microwear texture analysis. Journal of The Royal Society Interface,
723   16:20180957. doi: 10.1098/rsif.2018.0957.

724 Arsenault, R., and N. Owen-Smith. 2008. Resource partitioning by grass height among grazing ungulates does
725   not follow body size relation. Oikos, 117:1711–1717. doi: https://doi.org/10.1111/j.1600-
726   0706.2008.16575.x.

727 Bates, D., M. Mächler, B. Bolker, and S. Walker. 2015. Fitting linear mixed-effects models using lme4. Journal
728   of Statistical Software, 67:1–48. doi: doi:10.18637/jss.v067.i01.

729 Becker, D., and J. Tissier. 2020. Rhinocerotidae from the early middle Miocene locality Gračanica (Bugojno
730   Basin, Bosnia-Herzegovina). Palaeobiodiversity and Palaeoenvironments, 100:395–412. doi:
731   10.1007/s12549-018-0352-1.

732 Becker, D., P.-O. Antoine, and O. Maridet. 2013. A new genus of Rhinocerotidae (Mammalia, Perissodactyla)
733   from the Oligocene of Europe. ResearchGate, 2013:947–972. doi: 10.1080/14772019.2012.699007.

734 Bentaleb, I., C. Langlois, C. Martin, P. Iacumin, M. Carré, P.-O. Antoine, F. Duranthon, I. Moussa, J.-J. Jaeger,
735   and N. Barrett. 2006. Rhinocerotid tooth enamel 18O/16O variability between 23 and 12 Ma in
736   southwestern France. Comptes Rendus Geoscience, 338:172–179. doi: 10.1016/j.crte.2005.11.007.

737 Berlioz, É., D. S. Kostopoulos, C. Blondel, and G. Merceron. 2018. Feeding ecology of *Eucladoceros ctenoides*
738   as a proxy to track regional environmental variations in Europe during the early Pleistocene. Comptes
739   Rendus Palevol, 17:320–332. doi: 10.1016/j.crpv.2017.07.002.

740 Blanchet, F. G., K. Cazelles, and D. Gravel. 2020. Co-occurrence is not evidence of ecological interactions.
741   Ecology Letters, 23:1050–1063. doi: 10.1111/ele.13525.

742 Böhme, M. 2003. The Miocene Climatic Optimum: evidence from ectothermic vertebrates of Central Europe.
743   Palaeogeography, Palaeoclimatology, Palaeoecology, 195:389–401. doi: 10.1016/S0031-
744   0182(03)00367-5.

745 Böhme, M., A. Ilg, and M. Winklhofer. 2008. Late Miocene "washhouse" climate in Europe. Earth and Planetary
746   Science Letters, 275:393–401. doi: 10.1016/j.epsl.2008.09.011.

747 Böhme, M., M. Winklhofer, and A. Ilg. 2011. Miocene precipitation in Europe: Temporal trends and spatial
748   gradients. Palaeogeography, Palaeoclimatology, Palaeoecology, 304:212–218.

749 Böhmer, C., K. Heissig, and G. E. Rössner. 2016. Dental Eruption Series and Replacement Pattern in Miocene
750   *Prosantorhinus* (Rhinocerotidae) as Revealed by Macroscopy and X-ray: Implications for Ontogeny
751   and Mortality Profile. Journal of Mammalian Evolution, 23:265–279. doi: 10.1007/s10914-015-9313-x.

752 Bruch, A. A., D. Uhl, and V. Mosbrugger. 2007. Miocene climate in Europe — Patterns and evolution: A first
753   synthesis of NECLIME. Palaeogeography, Palaeoclimatology, Palaeoecology, 253:1–7. doi:
754   10.1016/j.palaeo.2007.03.030.

755 Butzmann, R., U. B. Göhlich, B. Bassler, and M. Krings. 2020. Macroflora and charophyte gyrogonites from the
756   middle Miocene Gračanica deposits in central Bosnia and Herzegovina. Palaeobiodiversity and
757   Palaeoenvironments, 100:479–491. doi: 10.1007/s12549-018-0356-x.

758 Calandra, I., U. B. Göhlich, and G. Merceron. 2008. How could sympatric megaherbivores coexist? Example of
759   niche partitioning within a proboscidean community from the Miocene of Europe. Die
760   Naturwissenschaften, 95:831–838. doi: 10.1007/s00114-008-0391-y.

761 Cerdeño, E. 1998. Diversity and evolutionary trends of the Family Rhinocerotidae (Perissodactyla).
762   Palaeogeography, Palaeoclimatology, Palaeoecology, 141:13–34. doi: https://doi.org/10.1016/S0031-
763   0182(98)00003-0.

764 Cerdeño, E., and M. Nieto. 1995. Changes in Western European Rhinocerotidae related to climatic variations.
765   Palaeogeography, Palaeoclimatology, Palaeoecology, 114:325–338.

766   Cerling, T. E., J. M. Harris, B. J. MacFadden, M. G. Leakey, J. Quade, V. Eisenmann, and J. R. Ehleringer.
767   1997. Global vegetation change through the Miocene/Pliocene boundary. Nature, 389:153–158.

768   Costeur, L., C. Guérin, and O. Maridet. 2012. Paléoécologie et paléoenvironnement du site miocène de Sansan;
769   p. 661–693. *In* S. Peigné and S. Sen (eds.), Mammifères de Sansan, Mémoires du Muséum national
770   d'Histoire naturelle. Vol. 203. Paris.

771   Damuth, J., and C. M. Janis. 2011. On the relationship between hypsodonty and feeding ecology in ungulate
772   mammals, and its utility in palaeoecology. Biological Reviews, 86:733–758. doi:
773   https://doi.org/10.1111/j.1469-185X.2011.00176.x.

774   Duranthon, F., P. O. Antoine, C. Bulot, and J. P. Capdeville. 1999. Le Miocène inférieur et moyen continental du
775   bassin d'Aquitaine Livret-guide de l'excursion des Journées Crouzel (10 et 11 juillet 1999). Bulletin de
776   La Société d'histoire Naturelle de Toulouse, 135:79–91.

777   Eronen, J. T., and G. E. Rössner. 2007. Wetland paradise lost: Miocene community dynamics in large
778   herbivorous mammals from the German Molasse Basin. Evolutionary Ecology Research, 9:471–494.

779   Fédération Dentaire Internationale. 1982. An epidemiological index of development defects of dental enamel
780   (DDE index). International Dental Journal, 42:411–426.

781   Fox, J., S. Weisberg, D. Adler, D. Bates, G. Baud-Bovy, S. Ellison, D. Firth, M. Friendly, G. Gorjanc, and S.
782   Graves. 2012. Package 'car.' Vienna: R Foundation for Statistical Computing,.

783   Fritz, H., P. Duncan, I. J. Gordon, and A. W. Illius. 2002. Megaherbivores influence trophic guilds structure in
784   African ungulate communities. Oecologia, 131:620–625.

785   Giaourtsakis, I., G. Theodorou, S. Roussiakis, A. Athanassiou, and G. Iliopoulos. 2006. Late Miocene horned
786   rhinoceroses (Rhinocerotinae, Mammlia) from Kerassia (Euboea, Greece). Neues Jahrbuch Für
787   Geologie Und Paläontologie - Abhandlungen, 239:367–398. doi: 10.1127/njgpa/239/2006/367.

788   Göhlich, U. B., and O. Mandic. 2020. Introduction to the special issue "The drowning swamp of Gračanica
789   (Bosnia-Herzegovina)—a diversity hotspot from the middle Miocene in the Bugojno Basin."
790   Palaeobiodiversity and Palaeoenvironments, 100:281–293. doi: 10.1007/s12549-020-00437-0.

791   Goodman, A. H., and J. C. Rose. 1990. Assessment of systemic physiological perturbations from dental enamel
792   hypoplasias and associated histological structures. American Journal of Physical Anthropology, 33:59–
793   110. doi: 10.1002/ajpa.1330330506.

794   Grine, F. E. 1986. Dental evidence for dietary differences in *Australopithecus* and *Paranthropus*: a quantitative
795   analysis of permanent molar microwear. Journal of Human Evolution, 15:783–822.

796   Heissig, K. 2012. Les Rhinocerotidae (Perissodactyla) de Sansan; p. 317–485. *In* S. Peigné and S. Sen (eds.),
797   Mammifères de Sansan. Vol. 203. Mémoires du Muséum national d'Histoire naturelle, Paris.

798   Hillman-Smith, A. K. K., N. R. Owen-Smith, J. L. Anderson, A. J. Hall-Martin, and J. P. Selaladi. 1986. Age
799   estimation of the white rhinoceros (*Ceratotherium simum*). Journal of Zoology, 210:355–377.

800   Hitchins, P. M. 1978. Age determination of the black rhinoceros (*Diceros bicornis* Linn.) in Zululand. South
801   African Journal of Wildlife Research, 8:71–80.

802   Hoffman, J. M., D. Fraser, and M. T. Clementz. 2015. Controlled feeding trials with ungulates: a new application
803   of in vivo dental molding to assess the abrasive factors of microwear. The Journal of Experimental
804   Biology, 218:1538–1547. doi: 10.1242/jeb.118406.

805   Holbourn, A., W. Kuhnt, M. Lyle, L. Schneider, O. Romero, and N. Andersen. 2014. Middle Miocene climate
806   cooling linked to intensification of eastern equatorial Pacific upwelling. Geology, 42:19–22.

807   Hullot, M., and P.-O. Antoine. 2020. Mortality curves and population structures of late early Miocene
808   Rhinocerotidae (Mammalia, Perissodactyla) remains from the Béon 1 locality of Montréal-du-Gers,

809   France. Palaeogeography, Palaeoclimatology, Palaeoecology, 558:109938. doi:
810   10.1016/j.palaeo.2020.109938.

811   Hullot, M., P.-O. Antoine, M. Ballatore, and G. Merceron. 2019. Dental microwear textures and dietary
812   preferences of extant rhinoceroses (Perissodactyla, Mammalia). Mammal Research, 64:397–409. doi:
813   10.1007/s13364-019-00427-4.

814   Hullot, M., Y. Laurent, G. Merceron, and P.-O. Antoine. 2021. Paleoecology of the Rhinocerotidae (Mammalia,
815   Perissodactyla) from Béon 1, Montréal-du-Gers (late early Miocene, SW France): Insights from dental
816   microwear texture analysis, mesowear, and enamel hypoplasia. Palaeontologia Electronica, 24:1–26.
817   doi: 10.26879/1163.

818   Hutchinson, G. E. 1959. Homage to Santa Rosalia or why are there so many kinds of animals? The American
819   Naturalist, 93:145–159.

820   Inigo, C., and E. Cerdeño. 1997. The *Hispanotherium matritense* (Rhinocerotidae) from Córcoles (Guadalajara,
821   Spain): Its contribution to the systematics of the Miocene Iranotheriina. Geobios, 30:243–266. doi:
822   10.1016/S0016-6995(97)80232-X.

823   Janis, C. 2008. An Evolutionary History of Browsing and Grazing Ungulates; p. 21–45. *In* I. J. Gordon and H. H.
824   T. Prins (eds.), The Ecology of Browsing and Grazing., . Ecological Studies Springer, Berlin,
825   Heidelberg doi: 10.1007/978-3-540-72422-3_2.

826   Janis, C. M. 1988. An estimation of tooth volume and hypsodonty indices in ungulate mammals, and the
827   correlation of these factors with dietary preferences. Memoires Du Museum National d' Histoire
828   Naturelle, serie C, 53:367–387.

829   Jardine, P. E., C. M. Janis, S. Sahney, and M. J. Benton. 2012. Grit not grass: Concordant patterns of early origin
830   of hypsodonty in Great Plains ungulates and Glires. Palaeogeography, Palaeoclimatology,
831   Palaeoecology, 365–366:1–10. doi: 10.1016/j.palaeo.2012.09.001.

832   Jones, D. B., and L. R. G. DeSantis. 2017. Dietary ecology of ungulates from the La Brea tar pits in southern
833   California: A multi-proxy approach. Palaeogeography, Palaeoclimatology, Palaeoecology, 466:110–
834   127. doi: 10.1016/j.palaeo.2016.11.019.

835   Kaiser, T. M. 2009. *Anchitherium aurelianense* (Equidae, Mammalia): a brachydont "dirty browser" in the
836   community of herbivorous large mammals from Sandelzhausen (Miocene, Germany). Paläontologische
837   Zeitschrift, 83:131.

838   Landman, M., D. S. Schoeman, and G. I. H. Kerley. 2013. Shift in Black Rhinoceros Diet in the Presence of
839   Elephant: Evidence for Competition? PLOS ONE, 8:e69771. doi: 10.1371/journal.pone.0069771.

840   Larramendi, A. 2015. Shoulder height, body mass, and shape of proboscideans. Acta Palaeontologica Polonica,
841   61:537–574.

842   Legendre, S., S. Montuire, O. Maridet, and G. Escarguel. 2005. Rodents and climate: A new model for
843   estimating past temperatures. Earth and Planetary Science Letters, 235:408–420. doi:
844   10.1016/j.epsl.2005.04.018.

845   Loponen, L. 2020. Diets of Miocene proboscideans from Eurasia, and their connection to environments and
846   vegetation. Master Thesis, University of Helsinki, Finland, 54 p.

847   Louail, M., S. Ferchaud, A. Souron, A. E. C. Walker, and G. Merceron. 2021. Dental microwear textures differ
848   in pigs with overall similar diets but fed with different seeds. Palaeogeography, Palaeoclimatology,
849   Palaeoecology, 572:110415. doi: 10.1016/j.palaeo.2021.110415.

850   MacFadden, B. 1992. Fossil Horses: Systematics, Paleobiology, and Evolution of the Family Equidae,
851   Cambridge University Press. New York, p.

852   Maridet, O., and S. Sen. 2012. Les Cricetidae (Rodentia) de Sansan; p. 29–65. *In* Mammifères de Sansan. Vol.

853   203. Mémoires du Muséum Paris.

854   Maridet, O., G. Escarguel, L. Costeur, P. Mein, M. Hugueney, and S. Legendre. 2007. Small mammal (rodents
855   and lagomorphs) European biogeography from the Late Oligocene to the mid Pliocene. Global Ecology
856   and Biogeography, 16:529–544. doi: https://doi.org/10.1111/j.1466-8238.2006.00306.x.

857   Martin, C., I. Bentaleb, and P.-O. Antoine. 2011. Pakistan mammal tooth stable isotopes show paleoclimatic and
858   paleoenvironmental changes since the early Oligocene. Palaeogeography Palaeoclimatology
859   Palaeoecology, 311:19–29. doi: 10.1016/j.palaeo.2011.07.010.

860   Mead, A. J. 1999. Enamel hypoplasia in Miocene rhinoceroses (*Teleoceras*) from Nebraska: evidence of severe
861   physiological stress. Journal of Vertebrate Paleontology, 19:391–397.

862   Merceron, G., A. Kallend, A. Francisco, M. Louail, F. Martin, C.-A. Plastiras, G. Thiery, and J.-R. Boisserie.
863   2021. Further away with dental microwear analysis: Food resource partitioning among Plio-Pleistocene
864   monkeys from the Shungura Formation, Ethiopia. Palaeogeography, Palaeoclimatology, Palaeoecology,
865   572:110414. doi: 10.1016/j.palaeo.2021.110414.

866   Merceron, G., A. Ramdarshan, C. Blondel, J.-R. Boisserie, N. Brunetiere, A. Francisco, D. Gautier, X. Milhet,
867   A. Novello, and D. Pret. 2016. Untangling the environmental from the dietary: dust does not matter.
868   Proc. R. Soc. B, 283 doi: 10.1098/rspb.2016.1032.

869   Mihlbachler, M. C., F. Rivals, N. Solounias, and G. M. Semprebon. 2011. Dietary change and evolution of
870   horses in North America. Science, 331:1178–1181. doi: 10.1126/science.1196166.

871   Niven, L. B., C. P. Egeland, and L. C. Todd. 2004. An inter-site comparison of enamel hypoplasia in bison:
872   implications for paleoecology and modeling Late Plains Archaic subsistence. Journal of Archaeological
873   Science, 31:1783–1794. doi: 10.1016/j.jas.2004.06.001.

874   Owen-Smith, N. R. 1988. Megaherbivores: The Influence of Very Large Body Size on Ecology. Cambridge
875   University Press, 392 p.

876   Prothero, D. R. 2005. The Evolution of North American Rhinoceroses. Cambridge University Press, 232 p.

877   Prothero, D. R., C. Guérin, and E. Manning. 1989. The history of the Rhinocerotoidea; p. 322–340. *In* D. R.
878   Prothero and R. M. Schoch (eds.), The Evolution of Perissodactyls. Oxford University Press, New
879   York.

880   Rivals, F., G. Semprebon, and A. Lister. 2012. An examination of dietary diversity patterns in Pleistocene
881   proboscideans (*Mammuthus*, *Palaeoloxodon*, and *Mammut*) from Europe and North America as
882   revealed by dental microwear. Quaternary International, 255:188–195. doi:
883   10.1016/j.quaint.2011.05.036.

884   Rivals, F., N. E. Prilepskaya, R. I. Belyaev, and E. M. Pervushov. 2020. Dramatic change in the diet of a late
885   Pleistocene *Elasmotherium* population during its last days of life: Implications for its catastrophic
886   mortality in the Saratov region of Russia. Palaeogeography, Palaeoclimatology, Palaeoecology,
887   556:109898. doi: 10.1016/j.palaeo.2020.109898.

888   Roohi, G., S. M. Raza, A. M. Khan, R. M. Ahmad, and M. Akhtar. 2015. Enamel Hypoplasia in Siwalik
889   Rhinocerotids and its Correlation with Neogene Climate. Pakistan Journal of Zoology, 47.

890   Rothschild, B. M., L. D. Martin, G. Lev, H. Bercovier, G. K. Bar-Gal, C. Greenblatt, H. Donoghue, M.
891   Spigelman, and D. Brittain. 2001. *Mycobacterium tuberculosis* Complex DNA from an Extinct Bison
892   Dated 17,000 Years before the Present. Clinical Infectious Diseases, 33:305–311. doi: 10.1086/321886.

893   Sabol, M., and M. Kováč. 2006. Badenian palaeoenvironment, faunal succession and biostratigraphy: a case
894   study from northern Vienna Basin, Devínska Nová Ves-Bonanza site (Western Carpathians, Slovakia).
895   Beiträge Zur Paläontologie, 30:415–425.

896   Scott, R. S., P. S. Ungar, T. S. Bergstrom, C. A. Brown, F. E. Grine, M. F. Teaford, and A. Walker. 2005. Dental

897   microwear texture analysis shows within-species diet variability in fossil hominins. Nature, 436:693–
898   695. doi: 10.1038/nature03822.

899   Scott, R. S., P. S. Ungar, T. S. Bergstrom, C. A. Brown, B. E. Childs, M. F. Teaford, and A. Walker. 2006.
900   Dental microwear texture analysis: technical considerations. Journal of Human Evolution, 51:339–349.
901   doi: 10.1016/j.jhevol.2006.04.006.

902   Semprebon, G. M., and F. Rivals. 2007. Was grass more prevalent in the pronghorn past? An assessment of the
903   dietary adaptations of Miocene to Recent Antilocapridae (Mammalia: Artiodactyla). Palaeogeography,
904   Palaeoclimatology, Palaeoecology, 253:332–347. doi: 10.1016/j.palaeo.2007.06.006.

905   Semprebon, G. M., P. J. Sise, and M. C. Coombs. 2011. Potential bark and fruit browsing as revealed by
906   stereomicrowear analysis of the peculiar clawed herbivores known as chalicotheres (Perissodactyla,
907   Chalicotherioidea). Journal of Mammalian Evolution, 18:33–55. doi: 10.1007/s10914-010-9149-3.

908   Semprebon, G. M., F. Rivals, and C. M. Janis. 2019. The Role of Grass vs. Exogenous Abrasives in the
909   Paleodietary Patterns of North American Ungulates. Frontiers in Ecology and Evolution, 7 doi:
910   10.3389/fevo.2019.00065.

911   Skinner, M. F., and J. D. Pruetz. 2012. Reconstruction of periodicity of repetitive linear enamel hypoplasia from
912   perikymata counts on imbricational enamel among dry-adapted chimpanzees (*Pan troglodytes verus*)
913   from Fongoli, Senegal. American Journal of Physical Anthropology, 149:468–482. doi:
914   10.1002/ajpa.22145.

915   Suckling, G., D. C. Elliott, and D. C. Thurley. 1986. The macroscopic appearance and associated histological
916   changes in the enamel organ of hypoplastic lesions of sheep incisor teeth resulting from induced
917   parasitism. Archives of Oral Biology, 31:427–439. doi: 10.1016/0003-9969(86)90016-6.

918   Tafforeau, P., I. Bentaleb, J.-J. Jaeger, and C. Martin. 2007. Nature of laminations and mineralization in
919   rhinoceros enamel using histology and X-ray synchrotron microtomography: potential implications for
920   palaeoenvironmental isotopic studies. Palaeogeography, Palaeoclimatology, Palaeoecology, 246:206–
921   227.

922   Tissier, J., P.-O. Antoine, and D. Becker. 2020. New material of *Epiaceratherium* and a new species of
923   *Mesaceratherium* clear up the phylogeny of early Rhinocerotidae (Perissodactyla). Royal Society Open
924   Science, 7:200633. doi: 10.1098/rsos.200633.

925   Tütken, T., T. M. Kaiser, T. Vennemann, and G. Merceron. 2013. Opportunistic Feeding Strategy for the Earliest
926   Old World Hypsodont Equids: Evidence from Stable Isotope and Dental Wear Proxies. PLOS ONE,
927   8:e74463. doi: 10.1371/journal.pone.0074463.

928   Upex, B., and K. Dobney. 2012. Dental enamel hypoplasia as indicators of seasonal environmental and
929   physiological impacts in modern sheep populations: a model for interpreting the zooarchaeological
930   record. Journal of Zoology, 287:259–268. doi: 10.1111/j.1469-7998.2012.00912.x.

931   Van der Made, J. 2003. Suoidea (Artiodactyla); p. 308–327. *In* Geology and paleontology of the Miocene Sinap
932   Formation, New York (Columbia University Press).

933   Venables, W. N., and B. D. Ripley. 2002. Modern Applied Statistics with S, Springer. New York, p.

934   Wasserstein, R. L., and N. A. Lazar. 2016. The ASA Statement on p-Values: Context, Process, and Purpose. The
935   American Statistician, 70:129–133. doi: 10.1080/00031305.2016.1154108.

936   Wasserstein, R. L., A. L. Schirm, and N. A. Lazar. 2019. Moving to a World Beyond "p < 0.05." The American
937   Statistician, 73:1–19. doi: 10.1080/00031305.2019.1583913.

938   Westerhold, T., N. Marwan, A. J. Drury, D. Liebrand, C. Agnini, E. Anagnostou, J. S. K. Barnet, S. M. Bohaty,
939   D. D. Vleeschouwer, F. Florindo, T. Frederichs, D. A. Hodell, A. E. Holbourn, D. Kroon, V. Lauretano,
940   K. Littler, L. J. Lourens, M. Lyle, H. Pälike, U. Röhl, J. Tian, R. H. Wilkens, P. A. Wilson, and J. C.
941   Zachos. 2020. An astronomically dated record of Earth's climate and its predictability over the last 66

942   million years. Science, 369:1383–1387. doi: 10.1126/science.aba6853.

943   Wickham, H. 2007. Reshaping data with the reshape package. Journal of Statistical Software, 21:1–20.

944   Wickham, H. 2011. ggplot2. Wiley Interdisciplinary Reviews: Computational Statistics, 3:180–185.

945   Wickham, H., R. François, L. Henry, and K. Müller. 2019. dplyr: A Grammar of Data Manipulation. R Package
946   Version 0.8.3, 13:2020.

947   Winkler, D. E., E. Schulz-Kornas, T. M. Kaiser, D. Codron, J. Leichliter, J. Hummel, L. F. Martin, M. Clauss,
948   and T. Tütken. 2020. The turnover of dental microwear texture: Testing the" last supper" effect in small
949   mammals in a controlled feeding experiment. Palaeogeography, Palaeoclimatology, Palaeoecology,
950   557:109930. doi: 10.1016/j.palaeo.2020.109930.

951   Xafis, A., J. Saarinen, K. Bastl, D. Nagel, and F. Grímsson. 2020. Palaeodietary traits of large mammals from
952   the middle Miocene of Gračanica (Bugojno Basin, Bosnia-Herzegovina). Palaeobiodiversity and
953   Palaeoenvironments, 100:457–477. doi: 10.1007/s12549-020-00435-2.

954   Zachos, J., M. Pagani, L. Sloan, E. Thomas, and K. Billups. 2001. Trends, rhythms, and aberrations in global
955   climate 65 Ma to present. Science, 292:686–693.

956